

1 Identification of FAM53C as a cytosolic-anchoring 2 inhibitory binding protein of the kinase DYRK1A

3

4 Yoshihiko Miyata^{1,*} & Eisuke Nishida^{1,2}

5

6 1 Department of Cell and Developmental Biology, Graduate School of Biostudies, Kyoto
7 University, Kyoto 606-8501, Japan

8 2 Present address: RIKEN Center for Biosystems Dynamics Research, Kobe 650-0047, Japan

9 *Corresponding author. Tel: +81-75-753-4231; E-mail: y Miyata@lif.kyoto-u.ac.jp

10

11 Abstract

12 The protein kinase DYRK1A encoded in human chromosome 21 is the major contributor to the multiple
13 symptoms observed in Down syndrome patients. In addition, DYRK1A malfunction is associated with
14 various other neurodevelopmental disorders such as autism spectrum disorder. Here we identified
15 FAM53C with no hitherto known biological function as a novel suppressive binding partner of DYRK1A.
16 FAM53C bound to the catalytic protein kinase domain of DYRK1A, whereas DCAF7/WDR68, the major
17 DYRK1A-binding protein, binds to the N-terminal domain of DYRK1A. The binding of FAM53C
18 inhibited autophosphorylation activity of DYRK1A and its kinase activity to an exogenous substrate
19 MAPT/Tau. FAM53C did not bind directly to DCAF7/WDR68, whereas DYRK1A tethered FAM53C
20 and DCAF7/WDR68 by binding concurrently to both of them, forming a tri-protein complex. DYRK1A
21 possesses a nuclear localization signal and accumulates in the nucleus when overexpressed in cells.
22 Co-expression of FAM53C induced cytoplasmic re-localization of DYRK1A, revealing the cytoplasmic
23 anchoring function of FAM53C to DYRK1A. Moreover, the binding of FAM53C to DYRK1A
24 suppressed the DYRK1A-dependent nuclear localization of DCAF7/WDR68. All the results show that
25 FAM53C binds to DYRK1A, suppresses its kinase activity, and anchors it in the cytoplasm. In addition,
26 FAM53C bound to the DYRK1A-related kinase DYRK1B with an Hsp90/Cdc37-independent manner.
27 The results explain for the first time why endogenous DYRK1A is distributed in the cytoplasm in normal
28 brain tissue. FAM53C-dependent regulation of the kinase activity and intracellular localization of
29 DYRK1A may play a significant role in gene expression regulation caused by normal and aberrant levels
30 of DYRK1A.

31

32 **Keywords: DCAF7/Down Syndrome/DYRK1A/FAM53C/Protein Kinase**

33

34 **Running Title: FAM53C binds and inhibits DYRK1A in the cytoplasm**

35

36

37 Introduction

38
39 DYRK1A (Dual-specificity tYrosine-phosphorylation Regulated Kinase 1A) is a proline-directed
40 serine/threonine protein kinase belonging to the CMGC family (Becker & Joost, 1999). The amino acid
41 sequence of the catalytic domain of DYRK1A is distantly related to that of MAP kinases (Miyata &
42 Nishida, 1999), implying that DYRK1A may play roles in certain cellular signal transduction systems.
43 DYRK1A phosphorylates various substrates both in the nucleus and cytoplasm, and consequently acts as a
44 regulator of the cell cycle, cell quiescence, and cell differentiation (Aranda et al, 2011; Becker & Sippl,
45 2011). DYRK1A is also involved in many other cellular processes such as cytoskeletal organization
46 (Ori-McKenney et al, 2016; Ryoo et al, 2007) and DNA damage response (Guard et al, 2019; Menon et al,
47 2019; Roewenstrunk et al, 2019). Human DYRK1A is encoded in the Down Syndrome Critical Region
48 (DSCR) in chromosome 21 (Galceran et al, 2003; Hämmerle et al, 2003) and higher expression of
49 DYRK1A is responsible for most of the phenotypes including intellectual disability of Down syndrome
50 patients (Altafaj et al, 2001). A role of DYRK1A has also been suggested in other pathological
51 conditions observed in Down syndrome patients, such as earlier onset of Alzheimer disease (Branca et al,
52 2017; Kimura et al, 2007), type 2 diabetes (Shen et al, 2015; Wang et al, 2015), and craniofacial
53 malformation (Blazek et al, 2015; McElyea et al, 2016; Redhead et al, 2023). In addition, recent studies
54 suggest that DYRK1A is also involved in several other neurodevelopmental disorders including ADHD
55 (Attention Deficit Hyperactivity Disorder) (Tian et al, 2019), ASD (Autism Spectrum Disorder) (De
56 Rubeis et al, 2014; O'Roak et al, 2012; van Bon et al, 2016), and DYRK1A-haploinsufficiency syndrome
57 (Courcet et al, 2012; Courraud et al, 2021; Duchon & Héroult, 2016). Altogether, it is evident that
58 DYRK1A plays a fundamental role in the process of neurodevelopment and neurofunction (Arbones et al,
59 2019; Atas-Ozcan et al, 2021). DYRK1A has thus recently emerged in the drug discovery field as an
60 attractive therapeutic target kinase. In contrast to many signaling kinases whose activities are regulated
61 by phosphorylation in the activation loop by upstream kinase-kinases, DYRK1A phosphorylates itself in
62 an activation loop tyrosine residue (Tyr321) during the transitional translation process, and this
63 autophosphorylation is essential for the constitutive serine/threonine-specific kinase activity of mature
64 DYRK1A for exogenous substrates (Himpel et al, 2001; Lochhead et al, 2005). The precise molecular
65 mechanism of DYRK1A regulating cellular physiology and human disease conditions remains largely
66 unknown.

67
68 Intracellular distribution of DYRK1A is of critical importance and has been a matter of considerable
69 debates. DYRK1A possesses nuclear localization signals (NLS) and thus DYRK1A accumulates inside
70 the nucleus when overexpressed in various cell lines (Álvarez et al, 2003; Becker et al, 1998; Miyata &
71 Nishida, 2011). Many transcription factors, including Nuclear Factor of Activated T-cells (NFAT),
72 FOXO1, and STAT3, are controlled by DYRK1A-dependent phosphorylation in the nucleus (Arron et al,
73 2006; Bhansali et al, 2021; Gwack et al, 2006). DYRK1A interacts with RNA polymerase II in the

74 nucleus and promotes its hyperphosphorylation in the C-terminal domain repeats through a phase
75 separation mechanism (Di Vona et al, 2015; Lu et al, 2018; Yu et al, 2019). In addition, DYRK1A
76 directly binds to chromatin regulatory regions to control gene expression (Di Vona et al, 2015; Li et al,
77 2018; Yu et al, 2019). These previous reports indicate that DYRK1A functions in the cell nucleus. On
78 the other hand, endogenous DYRK1A has been often observed in the cytoplasmic and cytoskeletal
79 fractions of cultured cells and natural brains of human and experimental animals (Aranda et al, 2008;
80 Ferrer et al, 2005; Martí et al, 2003; Nguyen et al, 2018; Wegiel et al, 2004). These observations suggest
81 that DYRK1A should have also cytoplasmic substrates. DYRK1A plays a critical role in activating the
82 mitochondrial import machinery by cytoplasmic phosphorylation of the import receptor TOM70 (Walter et
83 al, 2021), indicating that cytoplasmic function of DYRK1A is also physiologically important. Taking the
84 constitutive property of DYRK1A activity into account, the intracellular distribution of DYRK1A should
85 be strictly regulated by an unknown molecular mechanism.

86
87 We and others previously identified DCAF7 (DDB1 and CUL4 Associated Factor 7) [also called as
88 WDR68 (WD Repeat protein 68) or HAN11 (Human homolog of ANthocyanin regulatory gene 11), and
89 we use “DCAF7/WDR68” throughout the text hereafter] as a well-conserved major binding partner for
90 DYRK1A (Mazmanian et al, 2010; Miyata & Nishida, 2011; Morita et al, 2006; Skurat & Dietrich, 2004).
91 Structural analysis indicates that DCAF7/WDR68 forms a seven-propeller ring structure (Miyata et al,
92 2014) suggesting that DCAF7/WDR68 plays a role in tethering numerous binding partners on its structure
93 as other WD40-repeat proteins. In fact, several proteins, including IRS1, E1A oncoprotein, and RNA
94 polymerase II, have been shown to associate with DYRK1A via DCAF7/WDR68 (Frendo-Cumbo et al,
95 2022; Glenewinkel et al, 2016; Yu et al, 2019). Likewise, certain proteins may make complexes with
96 DCAF7/WDR68 via DYRK1A. Our earlier phospho-proteomic study obtained more than 250
97 associating partner candidates for DCAF7/WDR68 (Miyata et al, 2014), which may include
98 uncharacterized DYRK1A-binding proteins.

99
100 DYRK1B is the closest relative of DYRK1A with 85% amino acid identities in the catalytic protein
101 kinase domain (Becker et al, 1998), and most of DYRK1A-interacting partners including DCAF7/WDR68
102 are shared with DYRK1B (Miyata & Nishida, 2011; Varjosalo et al, 2013). On the other hand, Hsp90
103 (Heat Shock Protein 90) and Cdc37 (Cell Division Cycle protein 37) make a stable complex only with
104 DYRK1B, but not with DYRK1A (Miyata & Nishida, 2021). Identification of additional interacting
105 partners for DYRK1A and DYRK1B is of critical importance to understand the physiological roles of
106 these kinases.

107
108 In this study, we have identified FAM53C as a specific binding partner for DYRK1A and DYRK1B.
109 The catalytic kinase domain of DYRK1A was responsible for the FAM53C binding, while
110 DCAF7/WDR68 binds to the N-terminal domain of DYRK1A as previously shown (Glenewinkel et al,

111 2016; Miyata & Nishida, 2011). Hence, DYRK1A could simultaneously bind to both DCAF7/WDR68
112 and FAM53C forming a tri-protein complex, demonstrating a tethering function of DYRK1A. The
113 FAM53C binding suppressed the protein kinase activity of DYRK1A. In addition, the binding of
114 FAM53C induced cytoplasmic retention of DYRK1A, and the balance between the levels of DYRK1A
115 and FAM53C determined the intracellular distribution of DYRK1A. These results indicate that FAM53C
116 anchors DYRK1A in the cell cytoplasm in an inactive state. FAM53C may be a key molecule which
117 resolves the long-lasting controversial discrepancy of the intracellular distribution of DYRK1A between
118 overexpressed cell lines and the endogenous setting in human brain.

119

120

121 Results

122

123 Identification of FAM53C as a DCAF7/WDR68-DYRK1A interactor

124 DCAF7/WDR68 is a major binding partner of DYRK1A and DYRK1B (Glenewinkel et al, 2016;
125 Mazmanian et al, 2010; Miyata & Nishida, 2011; Morita et al, 2006; Ritterhoff et al, 2010; Skurat &
126 Dietrich, 2004). By a phospho-proteome analysis, we have previously identified proteins that are
127 physically associated with DCAF7/WDR68, directly or indirectly, along with their phosphorylation sites
128 (Miyata et al, 2014). The most prominent binding partner for DCAF7/WDR68 is a molecular chaperone
129 complex TriC/CCT (Miyata et al, 2014), and some of identified DCAF7/WDR68-associated partners, such
130 as actin and tubulin, may therefore interact with DCAF7/WDR68 indirectly via TRiC/CCT. Similarly,
131 DYRK1A-binding proteins should be possibly included in the DCAF7/WDR68-interactome network.
132 We identified FAM53C, FAMily with sequence similarity 53 member C, in the
133 DCAF7/WDR68-associated phosphoprotein list. The mass analysis identified nine peptides with one
134 phosphoserine each, and they covered 32.1% (126aa in 392aa) of FAM53C in total (Fig 1A). This result
135 indicates that FAM53C is an interacting partner for DCAF7/WDR68.

136 We then examined the BioPlex (biophysical interactions of ORFeome-based complexes) protein-protein
137 interaction database generated by immunoprecipitation of proteins stably expressed in human cell lines
138 followed by mass spectrometry (Huttlin et al, 2021; Huttlin et al, 2017). FAM53C (*orange*) is included
139 in the protein-protein interaction network of DYRK1A (Fig 1B, *upper panels*), DCAF7/WDR68 (Fig 1B,
140 *middle panels*), and DYRK1B (Fig 1B, *lower right panel*). In addition, DYRK1A (*blue*), DYRK1B
141 (*magenta*), and DCAF7/WDR68 (*yellow*) are all included in the FAM53C-interacting network (Fig 1B,
142 *lower left panel*). These protein-protein network analyses convincingly strengthen our result that
143 FAM53C is associated with DCAF7/WDR68 and also with DYRK1A and DYRK1B.

144

145 Human FAM53C consists of 392 amino acids and is rich in Ser (16%), Pro (14%), Leu (10%), and Arg
146 (9%), thus, a half of the protein consists of only the four amino acids, making FAM53C a low-complexity
147 sequence protein. Orthologous proteins of FAM53C are encoded in all the mammals examined with high
148 amino acid identities (99% in chimpanzee down to 80% in opossum and 59% in platypus), with lower
149 amino acid identities in lizard/snake (55%), frog (51-52%), turtle/crocodile (43-50%), shark/ray (38%),
150 bonny fish (33-35%), and chicken (33%), but not in cnidarians, nematode, insects, yeast, or plants,
151 suggesting that FAM53C may have vertebrate specific functions. Query for the Phyre2 structural
152 analysis (<http://www.sbg.bio.ic.ac.uk/phyre2/index.cgi>) of FAM53C resulted in no obvious similarity with
153 known protein folds. A predicted structure of FAM53C in AlphaFold Protein Structure Database
154 (<https://alphafold.com/>) shows that the majority of FAM53C structure is highly flexible and thus not
155 rigidly predictable. Prediction by the AlphaFold2 (alphafold2.ipynb: template mode=pdb70,
156 unpaired+paired) indicates that structures of only a limited number of small fragments of FAM53C can be
157 determined with high confidence (Fig 1C). In addition, secondary structure predictions with several

158 algorithms and intrinsically unstructured scores by IUPred2 (<https://iupred2a.elte.hu/>) both suggest that
159 this protein is composed of coil structures with intrinsically disordered regions throughout the molecule,
160 except short helices in the N- and C-terminal edges and several possible tiny beta-strands (Fig 1C).
161 According to these analyses, FAM53C seems to be a substantially disordered protein with a highly flexible
162 structure. Two related proteins FAM53A and FAM53B are encoded in the human genome and the amino
163 acid identities of FAM53C with FAM53A and FAM53B are 35% and 30%, respectively. FAM53C, as
164 well as FAM53A and FAM53B, has only very limited biochemical and physiological annotations for its
165 function so far.

166 The human protein atlas database (<https://www.proteinatlas.org/ENSG00000120709-FAM53C>)
167 indicates that FAM53C is expressed rich in brain and bone marrow, but also expressed in many human
168 tissues with low tissue specificity. The International Mouse Phenotyping Consortium database indicates
169 that FAM53C knock-out mice are viable, showing a phenotype classified as “Decreased exploration in
170 new environment” (<https://www.mousephenotype.org/data/genes/MGI:1913556>), suggesting that
171 FAM53C may play a role in neurodevelopment and/or neurological function.

172

173 **Binding of expressed and endogenous FAM53C with DYRK1A and DYRK1B**

174 As described above, we identified FAM53C as a DCAF7/WDR68-interacting protein, and large scale
175 interactome databases suggest that FAM53C may bind to DYRK1A and DYRK1B. We thus examined if
176 FAM53C makes complexes with DYRK1A and DYRK1B by co-immunoprecipitation experiments.
177 DYRK1A and DYRK1B were expressed as 3xFLAG-tagged proteins in mammalian cultured COS7 cells
178 (Fig 2B, *top*) with GFP-FAM53C (Fig 2B, *bottom*) and immunoprecipitated with anti-FLAG antibody (Fig
179 2A, *top*). The binding of GFP-FAM53C was examined by Western blotting with anti-GFP antibody (Fig
180 2A, *bottom*). The results indicated that FAM53C bound to and was co-immunoprecipitated with both
181 DYRK1A and DYRK1B.

182 To examine if endogenous FAM53C binds to DYRK1A and DYRK1B, we made an antibody against
183 FAM53C by immunizing a rabbit with a KLH-conjugated peptide, CQQDFGDLNLIEN,
184 corresponding to amino acids 377-392 (the last 16 amino acids of the C-terminal end) of orangutan
185 FAM53C. The sequence in this region is identical in FAM53C of almost all mammals from opossum to
186 primates. Very few exceptions with one amino acid change are observed in this region of FAM53C of
187 human (Q379R), hylobates (G383R), and echidna/platypus (C377S). Similar sequences are not
188 contained within any other mammalian proteins including the related family proteins FAM53A and
189 FAM53B. The antiserum was purified on an affinity column of resin conjugated with the antigen peptide.
190 The obtained antibody (Fig 3A, *top right panel*), but not preimmune serum (Fig 3A, *top left panel*),
191 recognized both monkey endogenous (*lane 1*) and exogenously expressed human FAM53C tagged with
192 3xFLAG (*lane 2*) or with GFP (*lane 3*). COS7 cells were then transfected with 3xFLAG-DYRK1A (Fig
193 3B, *lanes 3 & 4*) or 3xFLAG-DYRK1B (Fig 3B, *lanes 5 & 6*), and the binding of endogenous FAM53C
194 was examined by co-immunoprecipitation experiments. The binding of endogenous FAM53C was

195 evident in DYRK1A (*lane 4*) and DYRK1B (*lane 6*) immunoprecipitates, only when cells expressed
196 DYRK1A or DYRK1B, and immunoprecipitated with anti-FLAG antibody, but not with control antibody
197 (Fig 3B, *lanes 1-3, & 5*). The antibody against FAM53C recognized several protein bands in the extracts
198 (Fig 3A, *top right panel, lane 1*), and the uppermost band shown by an asterisk corresponds to the
199 FAM53C bound to DYRK1A and DYRK1B in Fig 3B, suggesting that this band is full length endogenous
200 FAM53C and a couple of other lower bands might be proteolytic fragments of FAM53C and/or other
201 proteins non-specifically recognized by the antibody. Altogether, these results show that FAM53C binds
202 to both DYRK1A and DYRK1B.

203

204 **FAM53C binds to the catalytic kinase domain of DYRK1A**

205 The FAM53C-binding domain in DYRK1A was next determined by co-immunoprecipitation experiments.
206 Wild type and deletion mutants of 3xFLAG-tagged DYRK1A were expressed (Fig 4D) with
207 GFP-FAM53C (Fig 4C) and the binding of FAM53C (Fig 4A) to immunoprecipitated DYRK1A (Fig 4B)
208 was determined by Western blotting with anti-GFP antibody. The kinase domain (aa156-479) alone
209 (DYRK1A(K), *lane 3*), but not the N-terminal (aa1-158) (DYRK1A(N), *lane 2*) nor C-terminal
210 (aa481-763) (DYRK1A(C), *lane 4*) domain of DYRK1A, bound to FAM53C. Deletion of the C-terminal
211 domain (DYRK1A(N+K), *lane 5*) or the N-terminal domain (DYRK1A(K+C), *lane 6*) of DYRK1A did
212 not abolish the FAM53C binding. Sufficient levels of GFP-FAM53C expression were observed in all the
213 extracts used for the co-immunoprecipitation assays (Fig 4C). The expression levels (Fig 4D) and the
214 amounts of immunoprecipitated proteins (Fig 4B) of DYRK1A fragments differed with each other, thus it
215 was difficult to accurately estimate the difference of binding levels of DYRK1A domains to FAM53C.
216 These results indicate that the catalytic kinase domain of DYRK1A, but not the N-terminal or C-terminal
217 domain, is responsible for the FAM53C binding. A possible contribution of other parts of DYRK1A
218 outside of the catalytic kinase domain for the FAM53C binding, however, cannot be excluded.

219

220 **Inhibition of the protein kinase activity of DYRK1A by the FAM53C binding**

221 The effect of the FAM53C binding to the catalytic kinase domain of DYRK1A on its protein kinase
222 activity was then examined. DYRK1A was expressed as a 3xFLAG-tagged protein in cultured COS7
223 cells with or without FAM53C co-expression and purified with anti-FLAG affinity resin followed by the
224 elution with the 3xFLAG peptide. An equal amount of DYRK1A, alone or in complex with FAM53C,
225 was then incubated in the presence of Mg²⁺-ATP with purified recombinant MAPT/Tau protein, a
226 well-established DYRK1A substrate (Woods et al, 2001). The levels of DYRK1A-dependent
227 phosphorylation of MAPT/Tau on Thr212 were quantified by Western blotting with a specific anti-pTau
228 Thr212 antibody. As shown in Fig 5A, MAPT/Tau phosphorylation by DYRK1A was much lower when
229 DYRK1A was in complex with FAM53C (*lane 6*) as compared to DYRK1A alone (*lane 5*). The total
230 amount of MAPT/Tau protein was not altered by the incubation for kinase reactions as shown by CBB
231 staining (Fig 5B). The electrophoretic mobilities of DYRK1A were affected when DYRK1A was

232 associated with FAM53C during the kinase reactions. In the absence of expressed FAM53C, a band with
233 a slower mobility (upper band) of DYRK1A was detected (Fig 5C, *lane 5*) while this upper band was not
234 observed when DYRK1A was associated with overexpressed FAM53C (Fig 5C, *lane 6*). The slower
235 mobility (the upper band) of DYRK1A in SDS-PAGE was previously ascribed to phosphorylated species
236 of DYRK1A (Alvarez et al, 2007). Therefore, the slower mobility DYRK1A observed after the kinase
237 reaction (*lane 5*) should be a result of DYRK1A autophosphorylation, and the absence of the
238 phosphorylated DYRK1A band indicates that DYRK1A lost its autophosphorylation activity when bound
239 to FAM53C. Specific binding of FAM53C to DYRK1A was detected by anti-FAM53C Western blotting
240 only when both proteins were concurrently expressed and DYRK1A was isolated with specific affinity
241 resin (Fig 5D, *lane 6*). The binding of endogenous FAM53C to DYRK1A as shown in Fig 3B was not
242 visible at this exposure. MAPT/Tau phosphorylation and the DYRK1A signal were not detected in
243 control conditions (Figs 5A & 5C, *lanes 1-4*). As shown in Figs 5E & 5G, the pTau (Thr212) signal and
244 the DYRK1A mobility up-shift required both Mg^{2+} and ATP (*lane 7-10*), validating that these are ascribed
245 to the Mg^{2+} /ATP-dependent protein phosphorylation reaction. The amounts of MAPT/Tau protein stayed
246 the same (Fig 5F). Taken together, these data indicate that DYRK1A possesses lower protein kinase
247 activity toward both itself and an exogenous substrate when it is associated with FAM53C.

248

249 **DYRK1A-dependent association of WDR68/DCAF7 with FAM53C**

250 Proteomic as well as co-immunoprecipitation experiments indicate that FAM53C makes a complex both
251 with DYRK1A and DCAF7/WDR68. We next set up an experiment to clarify if FAM53C directly binds
252 to DYRK1A, DCAF7/WDR68, or both. DCAF7/WDR68 was expressed in COS7 cells as an HA-tagged
253 protein with or without 3xFLAG-tagged FAM53C. In addition, GFP-tagged full length or deletion
254 mutants of DYRK1A was concurrently expressed. FAM53C and its associated proteins were
255 immunoprecipitated, and then the binding of DCAF7/WDR68 and DYRK1A was examined by Western
256 blotting. As in the case for the combination of 3xFLAG-DYRK1A and GFP-FAM53C (Figs 2 & 4),
257 3xFLAG-FAM53C and GFP-DYRK1A were found to be interacted (Fig 6B, *lane 4*). In addition,
258 DCAF7/WDR68 was included in the FAM53C-DYRK1A complex (Fig 6C, *lane 4*). DCAF7/WDR68
259 could not be co-immunoprecipitated with FAM53C in the absence of DYRK1A (Fig 6C, *lane 3*),
260 suggesting that FAM53C does not bind directly to DCAF7/WDR68. This result is in sharp contrast to
261 the binding of FAM53C to DYRK1A in the absence of exogenously expressed DCAF7/WDR68 (Figs 2-4).
262 Additional co-expression of DYRK1A induced the association between FAM53C and DCAF7/WDR68
263 (Fig 6C, compare *lanes 3 & 4*), indicating that DYRK1A is required for the binding of DCAF7/WDR68 to
264 FAM53C. Co-expression of DYRK1A-N domain, which binds to DCAF7/WDR68 but not to FAM53C
265 (Fig 6B, *lane 5*), could not induce the association of DCAF7/WDR68 with FAM53C (Fig 6C, *lane 5*).
266 Co-expression of DYRK1A-K domain, which does not bind to DCAF7/WDR68 but binds to FAM53C
267 (Fig 6B, *lane 6*), could not induce the association of DCAF7/WDR68 with FAM53C (Fig 6C, *lane 6*).
268 Contrarily, co-expression of DYRK1A-NK, which possesses both the DCAF7/WDR68-binding N-domain

269 and the FAM53C-binding K-domain, induced association of DCAF7/WDR68 with FAM53C (Fig 6C, *lane*
270 7) along with DYRK1A-NK (Fig 6B, *lane* 7). Expression levels of FLAG-FAM53C, GFP-DYRK1A,
271 and HA-DCAF7/WDR68 were shown in Fig 6D-6F. The amounts of immunoprecipitated FAM53C were
272 shown in Fig 6A. A schematic illustration of the expression of three proteins and FAM53C
273 immunocomplexes was shown in Fig 6G. These results indicate that DCAF7/WDR68 is not able to bind
274 directly to FAM53C without DYRK1A, and DCAF7/WDR68 binds to FAM53C in a DYRK1A-dependent
275 manner. In other words, DYRK1A brings DCAF7/WDR68 and FAM53C together with its N-domain
276 and K-domain, respectively.

277

278 **Intracellular distribution of FAM53C and DYRK1A**

279 To elucidate the intracellular distribution of FAM53C, we expressed GFP-tagged FAM53C in mammalian
280 cultured NIH-3T3 cells. The specific GFP-signal indicated that FAM53C localized in cytoplasmic
281 compartments of cells, and excluded from the nucleus (Fig 7B, *green*). 3xFLAG-DYRK1A when
282 expressed alone localized in the nucleus (Fig 7C, *magenta*), as we and others have shown previously in
283 several cell lines (Álvarez et al, 2003; Becker et al, 1998; Miyata & Nishida, 2011; Miyata & Nishida,
284 2021). Simultaneous expression of FAM53C with DYRK1A resulted in cytoplasmic re-distribution of
285 DYRK1A (Fig 7D, *magenta*) and DYRK1A co-localization with FAM53C (Figs 7D & 7E), suggesting
286 that FAM53C functions as a cytoplasmic anchoring protein for DYRK1A. The same conclusion was
287 obtained when we exchanged the tags for FAM53C and DYRK1A as follows. 3xFLAG-FAM53C
288 localized in the cytoplasm and excluded from the nucleus (Fig 7F, *magenta*), while GFP-DYRK1A
289 accumulated in the nucleus when expressed alone (Fig 7G, *green*). Co-expression of FAM53C with
290 DYRK1A induced cytoplasmic retention of DYRK1A (Fig 7H), resulting in co-localization of DYRK1A
291 with FAM53C in the cytoplasm (Figs 7H & 7I), again indicating the cytoplasmic anchoring function of
292 FAM53C toward DYRK1A. In same microscopic fields, we often observed that DYRK1A was excluded
293 from the nucleus of cells (*green*) where FAM53C expression levels (*magenta*) were high (Figs 7J & 7K,
294 *arrows*). On the other hand, DYRK1A remained in the nucleus of cells where only low or no FAM53C
295 was expressed (Figs 7J & 7K, *arrow heads*). This relationship between FAM53C expression levels and
296 DYRK1A localization shows that FAM53C regulates intracellular distribution of DYRK1A. Taken
297 together, these results indicate that FAM53C binding suppresses nuclear accumulation of DYRK1A in
298 cells and anchors DYRK1A in the cytoplasm.

299

300 **Tethering function of DYRK1A**

301 We have previously reported that DYRK1A binds to DCAF7/WDR68 and induces its nuclear
302 accumulation (Miyata & Nishida, 2011). We then examined if FAM53C modifies the DYRK1A-induced
303 nuclear localization of DCAF7/WDR68. When expressed alone, GFP-DCAF7/WDR68 localized both in
304 the cytoplasm and nucleus (Fig 8A, *green*). Co-expression of HA-DYRK1A which accumulated in the
305 nucleus (Fig 8B, *magenta*) induced nuclear co-localization of DCAF7/WDR68 with DYRK1A (Fig 8B,

306 *green*). Additional expression of 3xFLAG-FAM53C resulted in cytoplasmic re-localization of DYRK1A
307 (Fig 8D, *magenta*) as observed in Fig 7, and therefore, DYRK1A lost its ability to induce nuclear
308 re-localization of DCAF7/WDR68 (Fig 8D, *green*). Expression of 3xFLAG-FAM53C (Fig 8C, *blue*) in
309 the absence of DYRK1A did not influence the cellular localization of DCAF7/WDR68 (Fig 8C, *green*),
310 which agrees with the observation that FAM53C did not directly bind to DCAF7/WDR68 in the
311 co-immunoprecipitation assays (Fig 6). The same conclusion was obtained when we switched the tags.
312 3xFLAG-DCAF7/WDR68, when expressed alone, localized both in the cytoplasm and the nucleus (Fig 8E,
313 *blue*), and co-expression of HA-DYRK1A (accumulated in the nucleus as shown in Fig 8F, *magenta*)
314 induced nuclear co-localization of DCAF7/WDR68 (Fig 8F, *blue*) with DYRK1A. Expression of
315 GFP-FAM53C (Fig 8G, *green*) in the absence of DYRK1A did not influence the cellular localization of
316 DCAF7/WDR68 (Fig 8G, *blue*). Concurrent expression of GFP-FAM53C resulted in cytoplasmic
317 co-localization of both DYRK1A (Fig 8H, *magenta*) and DCAF7/WDR68 (Fig 8H, *blue*) with FAM53C
318 (Fig 8H, *green*). This result again indicates that FAM53C abrogates the ability of DYRK1A to anchor
319 DCAF7/WDR68 in the nucleus. Taken altogether, it is concluded that DYRK1A tethers DCAF7/WDR68
320 and FAM53C by binding both of them, and that FAM53C anchors DYRK1A and DYRK1A-associated
321 DCAF7/WDR68 in the cytoplasm.

322

323 **Binding of FAM53C and Hsp90/Cdc37 to DYRK1B**

324 The amino acid sequence identity is highest (85%) in the protein kinase catalytic domains of DYRK1A
325 and DYRK1B, and FAM53C binds to the protein kinase domain of DYRK1A (Fig 4). We have
326 previously shown that DYRK1B (but not DYRK1A) makes a stable complex with cellular molecular
327 chaperone Hsp90 and its co-chaperone Cdc37 (Miyata & Nishida, 2021), and the Hsp90/Cdc37 chaperone
328 system has been implicated in the maturation process of DYRK1B (Abu Jhaisha et al, 2017; Papenfuss et
329 al, 2022). Hsp90/Cdc37 recognizes the catalytic kinase domains of various protein kinases, thus, we next
330 examined the mutual relationship of DYRK1B-binding between Hsp90/Cdc37 and FAM53C. The
331 binding of FAM53C to DYRK1B was examined by co-immunoprecipitation experiments in the presence
332 or absence of an Hsp90-specific inhibitor Geldanamycin. Treatment of cells with Geldanamycin
333 abolished the binding of both Hsp90 (Fig 9C, compare *lanes 5 & 6, lanes 7 & 8*) and Cdc37 (Fig 9D,
334 compare *lanes 5 & 6, lanes 7 & 8*) to DYRK1B, in agreement with our previous investigation (Miyata &
335 Nishida, 2021). Even after the complete disruption of Hsp90/Cdc37-DYRK1B binding, the amount of
336 DYRK1B-associated FAM53C was not affected (Fig 9B, compare *lanes 7 & 8*). In addition,
337 overexpression of FAM53C did not disrupt the binding of Hsp90 and Cdc37 to DYRK1B (Figs 9C & 9D,
338 *lane 7*). We observed less Hsp90 and Cdc37 in the DYRK1B complexes from FAM53C-overexpressing
339 cells, however, this may be due to the decreased levels of expressed and immunoprecipitated DYRK1B by
340 the dual expression with FAM53C (Figs 9A & 9E, compare *lanes 5 and 7*), and quantification and
341 normalization with DYRK1B levels indicated that the amounts of associated Hsp90/Cdc37 per DYRK1B
342 was not significantly affected by the overexpression of FAM53C. The amounts of GFP-FAM53C, Hsp90,

343 and Cdc37 in the cell extracts were shown in Fig 9F, 9G, and 9H, respectively. These results indicate that
344 Hsp90/Cdc37 binding is not required for the FAM53C binding to DYRK1B and that Hsp90/Cdc37 does
345 not compete with FAM53C for binding to DYRK1B. The binding of Hsp90/Cdc37 and FAM53C may
346 require different parts in the protein kinase domain of DYRK1B and is mutually independent.
347

348 Discussion

349

350 **Tethering function and the protein interaction network of DYRK1A**

351 DCAF7/WDR68 is the primary binding partner for DYRK1A (Glenewinkel et al, 2016; Miyata & Nishida,
352 2011; Yu et al, 2019). Our phospho-proteomic analysis identified FAM53C as a protein that makes a
353 complex with DCAF7/WDR68 (Miyata & Nishida, 2021). Several other proteomic approaches have
354 identified FAM53C as a DYRK1A-interactor (Roewenstrunk et al, 2019) (Guard et al, 2019; Menon et al,
355 2019; Varjosalo et al, 2013; Viard et al, 2022). These results indicate that FAM53C associates in cells
356 with DYRK1A and/or DCAF7/WDR68. In this study, we directly show that DYRK1A binds to both
357 FAM53C and DCAF7/WDR68 simultaneously with its different regions on the molecule. Whereas
358 FAM53C bound to the protein kinase domain of DYRK1A (Fig 4), DCAF7/WDR68 binds to the
359 N-terminal domain of DYRK1A (Glenewinkel et al, 2016; Miyata & Nishida, 2011). DCAF7/WDR68
360 did not bind directly to FAM53C, but DYRK1A induced the association between DCAF7/WDR68 and
361 FAM53C by binding to both of them, forming the DCAF7/WDR68-DYRK1A-FAM53C tri-protein
362 complex. This result therefore indicates that our identification of FAM53C in the affinity-purified
363 DCAF7/WDR68 complex should be due to the binding of FAM53C to DCAF7/WDR68 through
364 endogenous DYRK1A in cells.

365

366 DYRK1A has been shown to associate in cells through DCAF7/WDR68 with several proteins including
367 MEKK1 (Ritterhoff et al, 2010), adenovirus E1A (Glenewinkel et al, 2016), and IRS1 (Frendo-Cumbo et al,
368 2022). In these cases, DCAF7/WDR68 works as a scaffold to stimulate the protein-protein interaction
369 between otherwise non-interacting partners. DCAF7/WDR68 is a WD40-repeat protein with a ring
370 structure consisted of seven beta-propellers, and proteins with this structure often function as bases for
371 protein-protein interactions (Stirnemann et al, 2010). On the other hand, our findings in this study
372 indicate that DYRK1A can also work as a scaffold to facilitate protein-protein interactions. Therefore,
373 the DYRK1A-DCAF7/WDR68 pair assembles many proteins using both DYRK1A and DCAF7/WDR68,
374 making this complex an important and efficient hub for many protein-protein interactions. Elucidation of
375 the whole DYRK1A protein network should be fundamental for understanding the physiological function
376 of DYRK1A in neurodevelopment and neurofunction at the molecular level.

377

378 We and others previously showed that DYRK1B, but not DYRK1A, makes stable complex with a set of
379 molecular chaperones, including Hsp90, its co-chaperone Cdc37, and Hsp70 (Abu Jhaisha et al, 2017;
380 Miyata & Nishida, 2021; Papenfuss et al, 2022). Hsp90/Cdc37 recognizes the catalytic domains of client
381 protein kinases as in the case of FAM53C, thus the relationship between the binding of FAM53C and
382 Hsp90/Cdc37 matters. Theoretically, FAM53C may bind to DYRK1B through Hsp90/Cdc37, however,
383 this possibility may be unlikely, because DYRK1A, which does not make a stable complex with
384 Hsp90/Cdc37, still binds to FAM53C. In addition, the complete dissociation of Hsp90/Cdc37 from

385 DYRK1B by the Geldanamycin treatment did not abolish nor enhance the binding of FAM53C to
386 DYRK1B (Fig 9), indicating that the Hsp90 binding to DYRK1B is dispensable and permissive for the
387 FAM53C binding.

388

389 **FAM53C phosphorylation**

390 Our phospho-proteomic analysis identified nine phosphorylation sites in FAM53C (Fig 1A), and all of
391 them are on serines (Ser86, Ser122, Ser162, Ser234, Ser247, Ser255, Ser273, Ser299, and Ser350).
392 Results by high throughput phospho-proteomic analyses in the PhosphoSite database
393 (<https://www.phosphosite.org/proteinAction.action?id=6364>) indicate that all the phosphoserines
394 identified in this study, except pSer-350, can be observed in human, mouse, and rat. In addition, the
395 PhosphoSite database indicates that pSer122 and pSer162 are sensitive to Torin1 (an inhibitor for mTOR)
396 and AZD1152/ZM447439 (inhibitors for Aurora kinase) / BI2536 (an inhibitor for PLK1), respectively.
397 It remains unclear if FAM53C is a direct substrate of these kinases in cells. Four of the identified
398 phosphorylation sites (pSer86, pSer162, pSer234, and pSer255) are immediately followed by a proline,
399 suggesting that these sites of FAM53C might be phosphorylated by certain proline-directed protein
400 kinases. Among them, the amino acid sequence surrounding pSer86 (RGNpSPKE) matches the
401 DYRK1A substrate consensus sequence (RXXpSP) (Aranda et al, 2011; Himpel et al, 2000). The amino
402 acid sequences surrounding pSer122 (RSLpSVP) and pSer273 (RSRpSQP) are consistent with the
403 consensus sequence motif (RXXpSXP) for phospho-dependent 14-3-3 binding (Pennington et al, 2018).
404 In fact, the BioPlex interactome database (Fig 1B, *lower left panel*) suggests interactions of FAM53C with
405 several 14-3-3 proteins including YWHAB(14-3-3 β), YWHAG(14-3-3 γ), YWHAH(14-3-3 η),
406 YQHAQ(14-3-3 θ), and YWHAZ(14-3-3 ζ). 14-3-3 proteins interact with numerous structurally and
407 functionally diverse targets and act as central hubs of cellular signaling networks (Pennington et al, 2018).
408 DYRK1A may therefore participate in a wide varieties of 14-3-3 dependent cellular signaling pathways
409 through FAM53C binding. A very recent proteomic interactome study with all 14-3-3 human paralogs
410 shows interaction of DYRK1A and FAM53C with five and six members out of seven 14-3-3 proteins
411 (Segal et al, 2023), respectively.

412

413 **FAM53C may function to keep DYRK1A in a kinase-inactive state in the cytoplasm**

414 Triplication of DYRK1A gene is responsible for many pathological phenotypes observed in Down
415 syndrome patients. Therefore, the regulation of DYRK1A function is of physiological and clinical
416 importance. Many low molecular weight compounds have been developed in the past decade as specific
417 DYRK1A inhibitors (Arbones et al, 2019; Duchon & Héroult, 2016; Feki & Hibaoui, 2018; Kumar et al,
418 2021; Stotani et al, 2016), however, only few endogenous proteins such as RanBPM and SPREAD (Li et
419 al, 2010; Zou et al, 2003) have been proposed to work inhibitory to DYRK1A. Here in this study, we
420 revealed that FAM53C suppresses the protein kinase activity of DYRK1A by binding to its catalytic
421 domain. The suppression was observed both in phosphorylation of a well-established DYRK1A

422 substrate MAPT/Tau and in autophosphorylation of DYRK1A itself. DYRK1A-dependent MAPT/Tau
423 phosphorylation is one of the molecular bases for the early onset of Alzheimer disease in majority of
424 Down syndrome patients (Ryoo et al, 2007) and DYRK1A inhibition is believed to be effective for
425 treatment of Alzheimer disease (Branca et al, 2017; Stotani et al, 2016). FAM53C, by suppressing
426 DYRK1A activity, may possibly also be involved in Alzheimer disease. DYRK1A is known to
427 autophosphorylate on a tyrosine residue in the activation loop and this autophosphorylation is required for
428 its maturation and full activity (Himpel et al, 2001; Lochhead et al, 2005). However, the
429 autophosphorylation shown in this study is different from the tyrosine-autophosphorylation, because the
430 tyrosine autophosphorylation is a one-off event during the translational process and the FAM53C-sensitive
431 autophosphorylation was observed in a post-maturation stage during the incubation of affinity-purified
432 DYRK1A with Mg^{2+} -ATP *in vitro*. The binding of FAM53C may interfere with the access of ATP or
433 substrates to DYRK1A, or inactivate DYRK1A kinase by inducing its conformational alteration.
434 Structural analysis of the FAM53C-DYRK1A complex may shed light on the molecular mechanism of the
435 DYRK1A inhibition by FAM53C.

436
437 DYRK1A encodes a bipartite nuclear localization signal in the N-terminal domain and accumulate in
438 the nucleus when exogenously over-expressed in various cell lines (Álvarez et al, 2003; Becker et al,
439 1998; Miyata & Nishida, 2011). However, many studies with various antibodies against DYRK1A have
440 indicated that endogenous DYRK1A resides within the cytoplasm of brain tissues and in cell lines (Aranda
441 et al, 2008; Ferrer et al, 2005; Martí et al, 2003; Nguyen et al, 2018; Wegiel et al, 2004). This
442 discrepancy have suggested that there may be an unveiled molecular mechanism responsible for anchoring
443 DYRK1A in the cytoplasm. DYRK1A regulates gene expression by phosphorylating nuclear substrates.
444 For example, DYRK1A-dependent phosphorylation of a transcription factor NFAT, which regulates
445 immuno-responsive, inflammatory, and developmental processes, induces its cytoplasmic re-localization
446 (Arron et al, 2006; Gwack et al, 2006). DYRK1A is also involved in transcriptional regulation by
447 interacting with histone acetyl transferase p300 and CBP (Li et al, 2018) and by phosphorylating the
448 C-terminal domain repeat of RNA polymerase II (Yu et al, 2019). Our results indicated that FAM53C
449 binds to DYRK1A and keeps DYRK1A inactive in the cytoplasm, suggesting that FAM53C prevents
450 DYRK1A from phosphorylating nuclear substrates. FAM53C is localized in the cytoplasm, and as the
451 amounts of FAM53C in cells increases, DYRK1A remains in the cytoplasm with FAM53C to a greater
452 extent (Fig 7). In the endogenous situation *in vivo*, DYRK1A and FAM53C levels remain in
453 physiological balance, therefore, FAM53C can finely regulate the intracellular distribution of DYRK1A,
454 appropriately keeping DYRK1A in the cytoplasm until needed. If DYRK1A is overexpressed beyond the
455 available endogenous FAM53C level, the excess FAM53C-free DYRK1A may translocate into the cell
456 nucleus and aberrantly phosphorylate nuclear proteins, leading to modified gene expression (Fig 10).
457 This may be one of the reasons why a mere 1.5-fold overexpression of DYRK1A can induce drastic
458 changes in gene expression and pathophysiological consequences in Down syndrome patients. FAM53C

459 knock-out mice do not reproduce all the DYRK1A trisomy phenotypes, indicating the involvement of
460 other molecular mechanisms, such as post-translational modifications or the binding of other interacting
461 partners, in the regulation of DYRK1A activity and localization. In addition, our findings are based on
462 the experiments conducted with overexpressed immortalized cell lines, therefore, the observed results may
463 not precisely represent the role of FAM53C in the impact of DYRK1A dosage effect in Down syndrome.
464

465 In conclusion, this study identified FAM53C as a binding protein of DYRK1A. DYRK1A
466 concurrently bound to both FAM53C and DCAF7/WDR68 via its kinase domain and N-terminal domain,
467 respectively, forming a tri-protein complex. FAM53C binding suppressed the protein kinase activity of
468 DYRK1A towards MAPT/Tau and its own autophosphorylation, anchoring the
469 DYRK1A-DCAF7/WDR68 complex in the cytoplasm in an inactive state. The amount of FAM53C in
470 cells determined the appropriate intracellular distribution of DYRK1A and DCAF7/WDR68.
471 Additionally, FAM53C bound to DYRK1B in an Hsp90/Cdc37-independent manner. These results
472 explain in part why endogenous DYRK1A in animal brain tissues is often observed in the cytoplasm
473 despite the strong tendency of DYRK1A nuclear localization. The identification of FAM53C as a
474 suppressive binding partner for DYRK1A sheds new light on the molecular mechanism of Down
475 syndrome caused by triplication of DYRK1A in human chromosome 21.
476
477

478 Materials and Methods

479

480 **Reagents and antibodies**

481 An antibody specific for FAM53C was raised in a rabbit against a KLH-conjugated peptide,
482 CQQDFGDLNLIEN, corresponding to amino acids 377-392 (C-terminal end) of orangutan FAM53C.
483 The antiserum was purified on an affinity column with the antigen peptide-conjugated resin. The peptide
484 synthesis, immunization, and affinity purification were performed at Cosmo Bio Co., Ltd. Anti-FLAG
485 antibody (M2), anti-FLAG (M2)-affinity resin, 3xFLAG peptide, and 3xFLAG-CMV7.1 vector were from
486 Sigma, anti-GFP antibody (JL8) was from Clontech, and anti-Cdc37 antibody (E-4) was from SantaCruz.
487 Anti-HA antibodies were from Roche (clone 12CA5 for Western blotting) or from SantaCruz (clone Y11
488 for immunofluorescent staining). Anti-Hsp90 antibody (Koyasu et al, 1986) and anti-DCAF7/WDR68
489 antibody (Miyata & Nishida, 2011) were described before. Geldanamycin was purchased from Life
490 Technologies Inc. or from InvivoGen and stock solution was prepared at 5 mM in DMSO.
491 pcDNA3-HA and pEGFP-C1Not vectors were previously described (Miyata et al, 1999; Miyata &
492 Nishida, 2011; Miyata & Nishida, 2021). Hoechst 33342 was from Molecular Probes.

493

494 **Isolation of human FAM53C cDNA**

495 A cDNA fragment encoding human FAM53C was isolated by amplifying with nested PCR from human
496 cDNA library plasmid (Takara). The oligonucleotide primer sequences used for the 1st PCR are
497 5'-CAAAGTGTGCAAGTCAAATCCTGG-3' (5' upstream) and 5'-CGGCTGGTTCTTCCGCCTC-3'
498 (antisense primer in the vector region). The oligonucleotide primer sequences used for the 2nd PCR are
499 5'-GCGGCCGCTATGATAACCCTGATCACTGAG-3' (*Not* I + 1st Met) and
500 5'-GCGGCCGCTTAGTTTTTCCTCAATCAAATTC-3' (3' end + *Not* I, antisense). As a result, the
501 amplified PCR fragment of FAM53C coding region contains a *Not* I site immediately 5' upstream of the
502 starting ATG and another *Not* I site 3' downstream of the stop codon. The obtained PCR fragment was
503 inserted into pCR2.1 Topo vector (Invitrogen) and the whole coding region was verified by direct
504 sequencing. The *Not* I fragment encoding the entire FAM53C coding region was purified by low-melting
505 gel electrophoresis. In the NCBI nucleotide database, three transcription variants are found for human
506 FAM53C and we obtained isoform 1 (392 amino acids) with our cloning strategy.

507

508 **Mammalian expression vectors for DYRK1A, DYRK1B, and FAM53C**

509 Expression plasmids for 3xFLAG-tagged DYRK1A(WT), DYRK1A(N), DYRK1A(K), DYRK1A(C),
510 DYRK1A(N+K), DYRK1A(K+C), and DYRK1B(WT) were previously described (Miyata & Nishida,
511 2011; Miyata & Nishida, 2021). *Not* I fragments encoding the N-terminal (N), the kinase domain (K),
512 and the N-terminal domain+the kinase domain (N+K) of DYRK1A were ligated into the *Not* I site of
513 pEGFPC1Not to obtain plasmids of GFP-fusion proteins for DYRK1A(N), DYRK1A(K), and
514 DYRK1A(N+K), respectively. HA-DYRK1A expression plasmid was previously described (Miyata &

515 Nishida, 2011). The *Not* I fragment of FAM53C was ligated into the *Not* I site of p3xFLAG-CMV7.1 or
516 pEGFP-C1Not to obtain plasmids for expression of 3xFLAG-tagged or GFP-tagged FAM53C.

517
518 **Expression in mammalian cells and immunoprecipitation experiments**
519 COS7 and NIH-3T3 cells were cultured in DMEM supplemented with 10% FCS at 37°C. Cells were
520 transfected with mammalian expression vectors by electroporation as described previously (Miyata et al,
521 1999; Miyata et al, 1997), or by lipofection with Lipofectamine LTX plus or with Lipofectamine 2000
522 according to the protocol supplied by the manufacture. Cell extracts were prepared as described before
523 (Miyata et al, 1999; Miyata et al, 1997). Extracts with equal amounts of proteins were incubated with 10
524 µl of anti-FLAG resin for 12h at 4°C. The immunocomplexes were washed, isolated, and FLAG-tagged
525 proteins were eluted and analyzed as described previously (Miyata et al, 2001; Miyata & Nishida, 2004).

526
527 **Immunofluorescent staining**
528 COS7 and NIH-3T3 cells were transfected with plasmids encoding GFP-, 3xFLAG-, or HA-tagged
529 proteins and cultured in 35mm dishes on glass cover slips. 24 hours later, cells were fixed with 10%
530 formaldehyde (37°C 20 min), stained with anti-FLAG- or anti-HA antibody, and observed with a
531 fluorescent microscope (Axiophot, Zeiss, or IX71, Olympus) essentially as described (Miyata & Nishida,
532 2004; Miyata & Nishida, 2021). For staining of the nuclei, cells were incubated with 1 µg/ml of Hoechst
533 33342, 3% BSA, 0.1% goat IgG in PBS at room temperature for 60 min. All the immunofluorescent
534 staining experiments were repeated with consistent results, and typical representative cell images are
535 shown.

536
537 **In vitro DYRK1A protein kinase assay**
538 The protein kinase activity of DYRK1A was determined *in vitro* with recombinant MAPT/Tau protein as
539 an exogenous substrate. A DNA fragment encoding human full length hT40 MAPT/Tau was obtained by
540 PCR with plasmid DNA encoding wild-type full-length hT40 MAPT/Tau as a template. The
541 oligonucleotide primer sequences used are 5'-GCGGCCGCCATGGCTGAGCCCCGCCAGGAG-3' (*Not* I
542 + 1st Met) and 5'- GCGGCCGCTCACAAACCCTGCTTGGCCAG-3' (3' end + *Not* I, antisense). As a
543 result, the amplified PCR fragment of MAPT/Tau coding region contains a *Not* I site immediately 5'
544 upstream of the starting ATG and another *Not* I site 3' downstream of the stop codon. The *Not* I fragment
545 was verified by direct sequencing and inserted into the *Not* I site of pGEX6P2 (Cytiva), and the expression
546 vector was introduced into an *Escherichia coli* strain BL21-CodonPlus (DE3)-RIL (Agilent). The
547 transformed bacterial cells were grown at 37°C until OD600 reached 0.7, and
548 isopropyl-β-D-thiogalactopyranoside (IPTG) was added at a final concentration of 0.5 mM to induce the
549 expression of GST-MAPT/Tau followed by 2h incubation at 22°C. The bacterial cells were collected by
550 a centrifugation (7,000 g 15 min 2°C), washed once with cold PBS, frozen at -80°C, and solubilized in
551 B-PER solution (Pierce) supplemented with 1/100 (v/v) of bacterial protease inhibitor cocktail (Sigma), 1

552 mM EDTA, and 0.5 M NaCl. The extract was clarified by a centrifugation (18,000 g 15 min 2°C) and
553 mixed with glutathione-Sepharose (Cytiva) for 4h followed by three times washes with PBS + TritonX100
554 (1%) and three times washes with cleavage buffer (50 mM Tris, 150 mM NaCl, 1 mM EDTA 1 mM DTT,
555 pH 7.0). The GST moiety of the fusion protein was removed by incubating with PreScission protease
556 (Cytiva) for 12h at 4°C, and released MAPT/Tau protein was purified with HiTrap CM Sepharose FF
557 (Cytiva) with a NaCl gradient (50-1,000 mM) in purification buffer (50 mM MES, 1 mM DTT, 1 mM
558 EDTA, pH 6.4). Eluted fractions containing MAPT/Tau protein were collected, desalted with a PD10
559 column (Cytiva) to 50 mM NaCl in the purification buffer, and concentrated by an Amicon Ultra-15 filter
560 unit (30,000Da cut-off, Millipore). The recombinant MAPT/Tau protein was >98% pure as revealed by
561 CBB staining.

562
563 3xFLAG-DYRK1A expressed in COS7 cells was affinity-purified as described above and incubated
564 with purified recombinant MAPT/Tau protein for 30 min at 30°C with gentle shaking for phosphorylation
565 reactions. Composition of the reaction mixture (20 µL) was 50 mM Hepes, 10 mM Tris, 1.25 mM MES,
566 81.25 mM NaCl, 2% glycerol, 10 mM MgCl₂, 5 mM ATP, 0.2% NP40, 0.225 mM DTT, 0.425 mM EDTA,
567 pH 7.4, containing 0.35 µg (17.5 µg/mL) MAPT/Tau. The reactions were stopped by adding
568 SDS-sample buffer followed by an incubation at 98°C for 5 min. DYRK1A-dependent phosphorylation
569 of Thr212 of MAPT/Tau protein was evaluated by Western blotting with anti-phospho Tau (Thr212)
570 antibody (Invitrogen, #44740G).

571
572 **Other procedures**

573 Sodium dodecyl sulfate-polyacrylamide gel electrophoresis (SDS-PAGE) was performed with 8% or 10%
574 acrylamide gels and BOLT MES (Invitrogen) or Tris-glycine SDS running buffer. Western blotting was
575 performed using polyvinylidene difluoride (PVDF) filter membranes (Millipore) for electro-transfer and
576 Blocking One (Nacalai Tesque) for blocking. Signals were developed with horseradish
577 peroxidase-conjugated secondary antibodies (GE Healthcare Bio-sciences) or peroxidase-conjugated
578 primary antibodies using Western Lightning Plus-ECL (PerkinElmer) and the chemiluminescent system
579 AI680 (GE Healthcare) as described (Miyata & Nishida, 2004). In some experiments, PVDF membrane
580 wetting was performed with ethanol instead of methanol, and we confirmed that this does not affect the
581 results. For all the Western blotting data, we repeated independent experiments and showed
582 representative images of obtained consistent results.

583
584
585

586 **Data availability**

587
588 This study does not contain deposited data in external repositories. Original data can be provided upon
589 request.

590
591 **Acknowledgements**
592 We thank T. Sakabe, T. Aoki, and M. Nakagawa for their excellent technical assistance. We thank Drs. B.
593 Chambraud and E. E. Baulieu (INSERM U1195, France) for providing us plasmid DNA encoding human
594 hT40 MAPT/Tau. This work was supported by Grants-in-Aid for Scientific Research from the Ministry
595 of Education, Culture, Sports, Science and Technology of Japan.

596
597 **Author contributions**
598 **Yoshihiko Miyata:** Conceptualization, methodology, investigation, visualization, project administration,
599 funding acquisition, writing –original draft, writing – review & editing.

600 **Eisuke Nishida:** Supervision, project administration, funding acquisition, resource, writing – review and
601 editing.

602
603 **Disclosure and competing interests statement**

604 The authors declare that they have no conflict of interest.

605
606

607 References

- 608
- 609 Abu Jhaisha S, Widowati EW, Kii I, Sonamoto R, Knapp S, Papadopoulos C, Becker W (2017) DYRK1B
610 mutations associated with metabolic syndrome impair the chaperone-dependent maturation of the
611 kinase domain. *Sci Rep* **7**: 6420
- 612 Altafaj X, Dierssen M, Baamonde C, Martí E, Visa J, Guimerà J, Oset M, González JR, Flórez J, Fillat C
613 *et al.* (2001) Neurodevelopmental delay, motor abnormalities and cognitive deficits in transgenic
614 mice overexpressing *Dyrk1A* (*minibrain*), a murine model of Down's syndrome. *Hum Mol Genet* **10**:
615 1915-1923
- 616 Alvarez M, Altafaj X, Aranda S, de la Luna S (2007) DYRK1A autophosphorylation on serine residue 520
617 modulates its kinase activity via 14-3-3 binding. *Mol Biol Cell* **18**: 1167-1178
- 618 Álvarez M, Estivill X, de la Luna S (2003) DYRK1A accumulates in splicing speckles through a novel
619 targeting signal and induces speckle disassembly. *J Cell Sci* **116**: 3099-3107
- 620 Aranda S, Alvarez M, Turró S, Laguna A, de la Luna S (2008) Sprouty2-mediated inhibition of fibroblast
621 growth factor signaling is modulated by the protein kinase DYRK1A. *Mol Cell Biol* **28**: 5899-5911
- 622 Aranda S, Laguna A, de la Luna S (2011) DYRK family of protein kinases: evolutionary relationships,
623 biochemical properties, and functional roles. *FASEB J* **25**: 449-462
- 624 Arbones ML, Thomazeau A, Nakano-Kobayashi A, Hagiwara M, Delabar JM (2019) DYRK1A and
625 cognition: A lifelong relationship. *Pharmacol Ther* **194**: 199-221
- 626 Arron JR, Winslow MM, Polleri A, Chang CP, Wu H, Gao X, Neilson JR, Chen L, Heit JJ, Kim SK *et al.*
627 (2006) NFAT dysregulation by increased dosage of DSCR1 and DYRK1A on chromosome 21.
628 *Nature* **441**: 595-600
- 629 Atas-Ozcan H, Brault V, Duchon A, Herault Y (2021) *Dyrk1a* from gene function in development and
630 physiology to dosage correction across life span in Down syndrome. *Genes* **12**: 1833
- 631 Becker W, Joost H-G (1999) Structural and functional characteristics of Dyrk, a novel subfamily of
632 protein kinases with dual specificity. *Prog Nucleic Acid Res Mol Biol* **62**: 1-17
- 633 Becker W, Sippl W (2011) Activation, regulation, and inhibition of DYRK1A. *FEBS J* **278**: 246-256
- 634 Becker W, Weber Y, Wetzel K, Eirmbter K, Tejedor FJ, Joost H-G (1998) Sequence characteristics,
635 subcellular localization, and substrate specificity of DYRK-related kinases, a novel family of dual
636 specificity protein kinases. *J Biol Chem* **273**: 25893-25902
- 637 Bhansali RS, Rammohan M, Lee P, Laurent AP, Wen Q, Suraneni P, Yip BH, Tsai YC, Jenni S, Bornhauser
638 B *et al.* (2021) DYRK1A regulates B cell acute lymphoblastic leukemia through phosphorylation of
639 FOXO1 and STAT3. *J Clin Invest* **131**: e135937
- 640 Blazek JD, Abeysekera I, Li J, Roper RJ (2015) Rescue of the abnormal skeletal phenotype in Ts65Dn
641 Down syndrome mice using genetic and therapeutic modulation of trisomic *Dyrk1a*. *Hum Mol Genet*
642 **24**: 5687-5696
- 643 Branca C, Shaw DM, Belfiore R, Gokhale V, Shaw AY, Foley C, Smith B, Hulme C, Dunckley T,

- 644 Meechoovet B *et al.* (2017) Dyrk1 inhibition improves Alzheimer's disease-like pathology. *Aging*
645 *Cell* **16**: 1146-1154
- 646 Courcet JB, Faivre L, Malzac P, Masurel-Paulet A, Lopez E, Callier P, Lambert L, Lemesle M, Thevenon J,
647 Gigot N *et al.* (2012) The DYRK1A gene is a cause of syndromic intellectual disability with severe
648 microcephaly and epilepsy. *J Med Genet* **49**: 731-736
- 649 Courraud J, Chater-Diehl E, Durand B, Vincent M, Del Mar Muniz Moreno M, Boujelbene I, Drouot N,
650 Genschik L, Schaefer E, Nizon M *et al.* (2021) Integrative approach to interpret DYRK1A variants,
651 leading to a frequent neurodevelopmental disorder. *Genet Med* **23**: 2150-2159
- 652 De Rubeis S, He X, Goldberg AP, Poultney CS, Samocha K, Cicek AE, Kou Y, Liu L, Fromer M, Walker
653 S *et al.* (2014) Synaptic, transcriptional and chromatin genes disrupted in autism. *Nature* **515**:
654 209-215
- 655 Di Vona C, Bezdan D, Islam AB, Salichs E, López-Bigas N, Ossowski S, de la Luna S (2015)
656 Chromatin-wide profiling of DYRK1A reveals a role as a gene-specific RNA polymerase II CTD
657 kinase. *Mol Cell* **57**: 506-520
- 658 Duchon A, Hérault Y (2016) DYRK1A, a dosage-sensitive gene involved in neurodevelopmental disorders,
659 is a target for drug development in Down syndrome. *Front Behav Neurosci* **10**: 104
- 660 Feki A, Hibaoui Y (2018) DYRK1A Protein, A Promising Therapeutic Target to Improve Cognitive
661 Deficits in Down Syndrome. *Brain Sci* **8**
- 662 Ferrer I, Barrachina M, Puig B, Martínez de Lagrán M, Martí E, Avila J, Dierssen M (2005) Constitutive
663 Dyrk1A is abnormally expressed in Alzheimer disease, Down syndrome, Pick disease, and related
664 transgenic models. *Neurobiol Dis* **20**: 392-400
- 665 Frendo-Cumbo S, Li T, Ammendolia DA, Coyaud E, Laurent EMN, Liu Y, Bilan PJ, Polevoy G, Raught B,
666 Brill JA *et al.* (2022) DCAF7 regulates cell proliferation through IRS1-FOXO1 signaling. *iScience*
667 **25**: 105188
- 668 Galceran J, de Graaf K, Tejedor FJ, Becker W (2003) The Mnb/Dyrk1A protein kinase: genetic and
669 biochemical properties. *J Neural Transm Suppl* **67**: 139-148
- 670 Glenewinkel F, Cohen MJ, King CR, Kaspar S, Bamberg-Lemper S, Mymryk JS, Becker W (2016) The
671 adaptor protein DCAF7 mediates the interaction of the adenovirus E1A oncoprotein with the protein
672 kinases DYRK1A and HIPK2. *Sci Rep* **6**: 28241
- 673 Guard SE, Poss ZC, Ebmeier CC, Pagratis M, Simpson H, Taatjes DJ, Old WM (2019) The nuclear
674 interactome of DYRK1A reveals a functional role in DNA damage repair. *Sci Rep* **9**: 6539
- 675 Gwack Y, Sharma S, Nardone J, Tanasa B, Iuga A, Srikanth S, Okamura H, Bolton D, Feske S, Hogan PG
676 *et al.* (2006) A genome-wide *Drosophila* RNAi screen identifies DYRK-family kinases as regulators
677 of NFAT. *Nature* **441**: 646-650
- 678 Hämmerle B, Elizalde C, Galceran J, Becker W, Tejedor FJ (2003) The Mnb/Dyrk1A protein kinase:
679 neurobiological functions and Down syndrome implications. *J Neural Transm Suppl* **67**: 129-137
- 680 Himpel S, Panzer P, Eirmbter K, Czajkowska H, Sayed M, Packman LC, Blundell T, Kentrup H,

- 681 Grötzinger J, Joost HG *et al.* (2001) Identification of the autophosphorylation sites and
682 characterization of their effects in the protein kinase DYRK1A. *Biochem J* **359**: 497-505
- 683 Himpel S, Tegge W, Frank R, Leder S, Joost HG, Becker W (2000) Specificity determinants of substrate
684 recognition by the protein kinase DYRK1A. *J Biol Chem* **275**: 2431-2438
- 685 Huttlin EL, Bruckner RJ, Navarrete-Perea J, Cannon JR, Baltier K, Gebreab F, Gygi MP, Thornock A,
686 Zarraga G, Tam S *et al.* (2021) Dual proteome-scale networks reveal cell-specific remodeling of the
687 human interactome. *Cell* **184**: 3022-3040.e3028
- 688 Huttlin EL, Bruckner RJ, Paulo JA, Cannon JR, Ting L, Baltier K, Colby G, Gebreab F, Gygi MP, Parzen
689 H *et al.* (2017) Architecture of the human interactome defines protein communities and disease
690 networks. *Nature* **545**: 505-509
- 691 Kimura R, Kamino K, Yamamoto M, Nuripa A, Kida T, Kazui H, Hashimoto R, Tanaka T, Kudo T,
692 Yamagata H *et al.* (2007) The DYRK1A gene, encoded in chromosome 21 Down syndrome critical
693 region, bridges between beta-amyloid production and tau phosphorylation in Alzheimer disease. *Hum*
694 *Mol Genet* **16**: 15-23
- 695 Koyasu S, Nishida E, Kadowaki T, Matsuzaki F, Iida K, Harada F, Kasuga M, Sakai H, Yahara I (1986)
696 Two mammalian heat shock proteins, HSP90 and HSP100, are actin-binding proteins. *Proc Natl Acad*
697 *Sci USA* **83**: 8054-8058
- 698 Kumar K, Suebsuwong C, Wang P, Garcia-Ocaña A, Stewart AF, DeVita RJ (2021) DYRK1A Inhibitors as
699 Potential Therapeutics for beta-Cell Regeneration for Diabetes. *J Med Chem* **64**: 2901-2922
- 700 Li D, Jackson RA, Yusoff P, Guy GR (2010) Direct Association of Sprouty-related Protein with an EVH1
701 Domain (SPRED) 1 or SPRED2 with DYRK1A Modifies Substrate/Kinase Interactions. *J Biol Chem*
702 **285**: 35374-35385
- 703 Li S, Xu C, Fu Y, Lei PJ, Yao Y, Yang W, Zhang Y, Washburn MP, Florens L, Jaiswal M *et al.* (2018)
704 DYRK1A interacts with histone acetyl transferase p300 and CBP and localizes to enhancers. *Nucleic*
705 *Acids Res* **46**: 11202-11213
- 706 Lochhead PA, Sibbet G, Morrice N, Cleghon V (2005) Activation-loop autophosphorylation is mediated
707 by a novel transitional intermediate form of DYRKs. *Cell* **121**: 925-936
- 708 Lu H, Yu D, Hansen AS, Ganguly S, Liu R, Heckert A, Darzacq X, Zhou Q (2018) Phase-separation
709 mechanism for C-terminal hyperphosphorylation of RNA polymerase II. *Nature* **558**: 318-323
- 710 Martí E, Altafaj X, Dierssen M, de la Luna S, Fotaki V, Alvarez M, Pérez-Riba M, Ferrer I, Estivill X
711 (2003) Dyrk1A expression pattern supports specific roles of this kinase in the adult central nervous
712 system. *Brain Res* **964**: 250-263
- 713 Mazmanian G, Kovshilovsky M, Yen D, Mohanty A, Mohanty S, Nee A, Nissen RM (2010) The zebrafish
714 *dyrk1b* gene is important for endoderm formation. *Genesis* **48**: 20-30
- 715 McElyea SD, Starbuck JM, Tumbleson-Brink DM, Harrington E, Blazek JD, Ghoneima A, Kula K, Roper
716 RJ (2016) Influence of prenatal EGCG treatment and Dyrk1a dosage reduction on craniofacial
717 features associated with Down syndrome. *Hum Mol Genet* **25**: 4856-4869

- 718 Menon VR, Ananthapadmanabhan V, Swanson S, Saini S, Sesay F, Yakovlev V, Florens L, DeCaprio JA,
719 Washburn MP, Dozmorov M *et al.* (2019) DYRK1A regulates the recruitment of 53BP1 to the sites of
720 DNA damage in part through interaction with RNF169. *Cell Cycle* **18**: 531-551
- 721 Miyata Y, Akashi M, Nishida E (1999) Molecular cloning and characterization of a novel member of the
722 MAP kinase superfamily. *Genes Cells* **4**: 299-309
- 723 Miyata Y, Chambraud B, Radanyi C, Leclerc J, Lebeau M-C, Renoir J-M, Shirai R, Catelli M-G, Yahara I,
724 Baulieu E-E (1997) Phosphorylation of the immunosuppressant FK506-binding protein FKBP52 by
725 casein kinase II (CK2): Regulation of HSP90-binding activity of FKBP52. *Proc Natl Acad Sci USA*
726 **94**: 14500-14505
- 727 Miyata Y, Ikawa Y, Shibuya M, Nishida E (2001) Specific association of a set of molecular chaperones
728 including HSP90 and Cdc37 with MOK, a member of the MAP kinase superfamily. *J Biol Chem* **276**:
729 21841-21848
- 730 Miyata Y, Nishida E (1999) Distantly related cousins of MAP kinase: Biochemical properties and possible
731 physiological functions. *Biochem Biophys Res Commun* **266**: 291-295
- 732 Miyata Y, Nishida E (2004) CK2 controls multiple protein kinases by phosphorylating a kinase-targeting
733 molecular chaperone Cdc37. *Mol Cell Biol* **24**: 4065-4074
- 734 Miyata Y, Nishida E (2011) DYRK1A binds to an evolutionarily conserved WD40-repeat protein WDR68
735 and induces its nuclear translocation. *Biochim Biophys Acta-Mol Cell Res* **1813**: 1728-1739
- 736 Miyata Y, Nishida E (2021) Protein quality control of DYRK family protein kinases by the Hsp90-Cdc37
737 molecular chaperone. *Biochim Biophys Acta-Mol Cell Res* **1868**: 119081
- 738 Miyata Y, Shibata T, Aoshima M, Tsubata T, Nishida E (2014) The molecular chaperone TRiC/CCT binds
739 to the Trp-Asp 40 (WD40) repeat protein WDR68 and promotes its folding, protein kinase DYRK1A
740 binding, and nuclear accumulation. *J Biol Chem* **289**: 33320-33332
- 741 Morita K, Lo Celso C, Spencer-Dene B, Zouboulis CC, Watt FM (2006) HAN11 binds mDia1 and
742 controls GII1 transcriptional activity. *J Dermatol Sci* **44**: 11-20
- 743 Nguyen TL, Duchon A, Manousopoulou A, Loaëc N, Villiers B, Pani G, Karatas M, Mechling AE, Harsan
744 LA, Limanton E *et al.* (2018) Correction of cognitive deficits in mouse models of Down syndrome by
745 a pharmacological inhibitor of DYRK1A. *Dis Model Mech* **11**: dmm035634
- 746 O'Roak BJ, Vives L, Girirajan S, Karakoc E, Krumm N, Coe BP, Levy R, Ko A, Lee C, Smith JD *et al.*
747 (2012) Sporadic autism exomes reveal a highly interconnected protein network of de novo mutations.
748 *Nature* **485**: 246-250
- 749 Ori-McKenney KM, McKenney RJ, Huang HH, Li T, Meltzer S, Jan LY, Vale RD, Wiita AP, Jan YN
750 (2016) Phosphorylation of beta-Tubulin by the Down Syndrome Kinase, Minibrain/DYRK1a,
751 Regulates Microtubule Dynamics and Dendrite Morphogenesis. *Neuron* **90**: 551-563
- 752 Papenfuss M, Lützwow S, Wilms G, Babendreyer A, Flaßhoff M, Kunick C, Becker W (2022) Differential
753 maturation and chaperone dependence of the paralogous protein kinases DYRK1A and DYRK1B. *Sci*
754 *Rep* **12**: 2393

- 755 Pennington KL, Chan TY, Torres MP, Andersen JL (2018) The dynamic and stress-adaptive signaling hub
756 of 14-3-3: emerging mechanisms of regulation and context-dependent protein-protein interactions.
757 *Oncogene* **37**: 5587-5604
- 758 Redhead Y, Gibbins D, Lana-Elola E, Watson-Scales S, Dobson L, Krause M, Liu KJ, Fisher EMC, Green
759 JBA, Tybulewicz VLJ (2023) Craniofacial dysmorphology in Down syndrome is caused by increased
760 dosage of Dyrk1a and at least three other genes. *Development* **150**: dev201077
- 761 Ritterhoff S, Farah CM, Grabitzki J, Lochnit G, Skurat AV, Schmitz ML (2010) The WD40-repeat protein
762 Han11 functions as a scaffold protein to control HIPK2 and MEKK1 kinase functions. *EMBO J* **29**:
763 3750-3761
- 764 Roewenstrunk J, Di Vona C, Chen J, Borrás E, Dong C, Arató K, Sabidó E, Huen MSY, de la Luna S
765 (2019) A comprehensive proteomics-based interaction screen that links DYRK1A to RNF169 and to
766 the DNA damage response. *Sci Rep* **9**: 6014
- 767 Ryoo SR, Jeong HK, Radnaabazar C, Yoo JJ, Cho HJ, Lee HW, Kim IS, Cheon YH, Ahn YS, Chung SH *et*
768 *al.* (2007) DYRK1A-mediated hyperphosphorylation of Tau. A functional link between Down
769 syndrome and Alzheimer disease. *J Biol Chem* **282**: 34850-34857
- 770 Segal D, Maier S, Mastromarco GJ, Qian WW, Nabeel-Shah S, Lee H, Moore G, Lacoste J, Larsen B, Lin
771 ZY *et al.* (2023) A central chaperone-like role for 14-3-3 proteins in human cells. *Mol Cell* **83**:
772 974-993 e915
- 773 Shen W, Taylor B, Jin Q, Nguyen-Tran V, Meeusen S, Zhang YQ, Kamireddy A, Swafford A, Powers AF,
774 Walker J *et al.* (2015) Inhibition of DYRK1A and GSK3B induces human beta-cell proliferation. *Nat*
775 *Commun* **6**: 8372
- 776 Skurat AV, Dietrich AD (2004) Phosphorylation of Ser640 in muscle glycogen synthase by DYRK family
777 protein kinases. *J Biol Chem* **279**: 2490-2498
- 778 Stirnimann CU, Petsalaki E, Russell RB, Müller CW (2010) WD40 proteins propel cellular networks.
779 *Trends Biochem Sci* **35**: 565-574
- 780 Stotani S, Giordanetto F, Medda F (2016) DYRK1A inhibition as potential treatment for Alzheimer's
781 disease. *Future Med Chem* **8**: 681-696
- 782 Tian T, Zhang Y, Wu T, Yang L, Chen C, Li N, Li Y, Xu S, Fu Z, Cui X *et al.* (2019) miRNA profiling in
783 the hippocampus of attention-deficit/hyperactivity disorder rats. *J Cell Biochem* **120**: 3621-3629
- 784 van Bon BW, Coe BP, Bernier R, Green C, Gerds J, Witherspoon K, Kleefstra T, Willemsen MH, Kumar
785 R, Bosco P *et al.* (2016) Disruptive de novo mutations of DYRK1A lead to a syndromic form of
786 autism and ID. *Mol Psychiatry* **21**: 126-132
- 787 Varjosalo M, Keskitalo S, Van Drogen A, Nurkkala H, Vichalkovski A, Aebersold R, Gstaiger M (2013)
788 The protein interaction landscape of the human CMGC kinase group. *Cell Rep* **3**: 1306-1320
- 789 Viard J, Loe-Mie Y, Daudin R, Khelifaoui M, Plancon C, Boland A, Tejedor F, Haganir RL, Kim E,
790 Kinoshita M *et al.* (2022) Chr21 protein-protein interactions: enrichment in proteins involved in
791 intellectual disability, autism, and late-onset Alzheimer's disease. *Life Sci Alliance* **5**: e202101205

- 792 Walter C, Marada A, Suhm T, Ernsberger R, Muders V, Kücükköse C, Sánchez-Martín P, Hu Z, Aich A,
793 Lorocho S *et al.* (2021) Global kinome profiling reveals DYRK1A as critical activator of the human
794 mitochondrial import machinery. *Nat Commun* **12**: 4284
- 795 Wang P, Alvarez-Perez JC, Felsenfeld DP, Liu H, Sivendran S, Bender A, Kumar A, Sanchez R, Scott DK,
796 Garcia-Ocaña A *et al.* (2015) A high-throughput chemical screen reveals that harmine-mediated
797 inhibition of DYRK1A increases human pancreatic beta cell replication. *Nat Med* **21**: 383-388
- 798 Wegiel J, Kuchna I, Nowicki K, Frackowiak J, Dowjat K, Silverman WP, Reisberg B, DeLeon M,
799 Wisniewski T, Adayev T *et al.* (2004) Cell type- and brain structure-specific patterns of distribution
800 of minibrain kinase in human brain. *Brain Res* **1010**: 69-80
- 801 Woods YL, Cohen P, Becker W, Jakes R, Goedert M, Wang X, Proud CG (2001) The kinase DYRK
802 phosphorylates protein-synthesis initiation factor eIF2Bepsilon at Ser539 and the
803 microtubule-associated protein tau at Thr212: potential role for DYRK as a glycogen synthase kinase
804 3-priming kinase. *Biochem J* **355**: 609-615
- 805 Yu D, Cattoglio C, Xue Y, Zhou Q (2019) A complex between DYRK1A and DCAF7 phosphorylates the
806 C-terminal domain of RNA polymerase II to promote myogenesis. *Nucleic Acids Res* **47**: 4462-4475
- 807 Zou Y, Lim S, Lee K, Deng X, Friedman E (2003) Serine/threonine kinase Mirk/Dyrk1B is an inhibitor of
808 epithelial cell migration and is negatively regulated by the Met adaptor Ran-binding protein M. *J Biol*
809 *Chem* **278**: 49573-49581
- 810
- 811

812 **Figure legends**

813

814 **Figure 1. Identification of FAM53C as an interactor candidate for DCAF7/WDR68 and DYRK1A**

815

816 **A.** Phospho-proteomic analysis of binding proteins of DCAF7/WDR68 exogenously expressed in COS7
817 cells identified nine phosphopeptides (underlined orange boxes) corresponding to FAM53C. The
818 amino acid sequence of human FAM53C is shown with identified phosphorylation sites (shown in
819 green with amino acid numbers).

820 **B.** BioPlex protein-protein interaction network analysis. The database was analyzed with DYRK1A
821 (*upper panels*, in HEK293T [*left*] or HCT116 [*right*]), DCAF7/WDR68 (*middle panels*, in HEK293T
822 [*left*] or HCT116 [*right*]), FAM53C (*lower left panel* in HEK293T), and DYRK1B (*lower right panel*
823 in HEK293T) as queries (located in the center of the networkgrams). Identified interacting partners
824 are shown and FAM53C (*orange*), DCAF7/WDR68 (*yellow*), DYRK1A (*blue*), and DYRK1B
825 (*magenta*) are color-highlighted. Proteins with circles indicate baits, and proteins with diamonds
826 indicate prey. The arrow heads show the bait-to-prey direction.

827 **C.** Structural characterization of FAM53C. Structural prediction of FAM53C by AlphaFold2 (*upper*
828 *panel*) and the intrinsically disordered tendency score of FAM53C by IUPred2 (*lower panel*) are
829 shown.

830

831 **Figure 2. Association of FAM53C with DYRK1A and DYRK1B**

832

833 DYRK1A and DYRK1B were expressed as 3xFLAG-tagged proteins with GFP-tagged FAM53C in COS7
834 cells. DYRK1A and DYRK1B were immunoprecipitated with resin conjugated with anti-FLAG
835 antibody and protein complexes were analyzed by SDS-PAGE/Western blotting.

836

837 **A.** The amounts of DYRK1A, DYRK1B (*upper panel*), and FAM53C (*lower panel*) in the
838 immunocomplexes were shown by Western blotting. *Lane 1*, Control; *lane 2*, DYRK1A; *lane 3*,
839 DYRK1B.

840 **B.** The amounts of DYRK1A, DYRK1B (*upper panel*), and FAM53C (*lower panel*) in the extracts were
841 shown by Western blotting. *Lane 1*, Control; *lane 2*, DYRK1A; *lane 3*, DYRK1B. FAM53C were
842 transfected in *lanes 1-3*.

843

844 **Figure 3. Binding of endogenous FAM53C with DYRK1A and DYRK1B**

845

846 **A.** COS7 cells (*lane 1*, control) were transfected with 3xFLAG-FAM53C (*lane 2*) or GFP-FAM53C (*lane*
847 *3*). Total cell lysates were prepared and examined by Western blotting with indicated antibodies as
848 follows. *Top left*, control pre-immune serum; *Top right*, C-terminal peptide-directed FAM53C

849 antibody (extracts in *lanes 2 & 3* in this panel were x100 diluted to avoid signal saturation. The
850 asterisk indicates the position of full length endogenous FAM53C); *Bottom left*, anti-FLAG antibody,
851 showing the expression of 3xFLAG-FAM53C; *Bottom right*, anti-GFP antibody, showing the
852 expression of GFP-FAM53C.

853 **B.** COS7 cells were transfected with 3xFLAG-tagged DYRK1A or DYRK1B and the
854 co-immunoprecipitation of endogenous FAM53C with DYRK1A and DYRK1B was examined by
855 Western blotting. *Lane 1*, control IgG-immunoprecipitate from non-transfected control cells; *lane 2*,
856 anti-FLAG immunoprecipitate from non-transfected control cells; *lane 3*, control
857 IgG-immunoprecipitate from 3xFLAG-DYRK1A-transfected cells; *lane 4*,
858 anti-FLAG-immunoprecipitate from 3xFLAG-DYRK1A-transfected cells; *lane 5*, control
859 IgG-immunoprecipitate from 3xFLAG-DYRK1B-transfected cells; *lane 6*,
860 anti-FLAG-immunoprecipitate from 3xFLAG-DYRK1B-transfected cells. Western blotting images
861 with the anti-FAM53C antibody (*upper panels*) and with anti-FLAG antibody (*lower panels*) are
862 shown.

863

864 **Figure 4. Identification of the FAM53C binding domain in DYRK1A**

865

866 3xFLAG-DYRK1A (wild type or deletion mutants) and GFP-FAM53C were expressed in COS7 cells and
867 the binding of FAM53C to DYRK1A was examined by co-immunoprecipitation experiments. *Lane 1*,
868 DYRK1A(WT); *lane 2*, DYRK1A(N); *lane 3*, DYRK1A(K); *lane 4*, DYRK1A(C); *lane 5*,
869 DYRK1A(N+K); *lane 6*, DYRK1A(K+C).

870

871 **A.** Western blotting of immunoprecipitates with anti-GFP antibody for detection of DYRK1A-bound
872 FAM53C.

873 **B.** Western blotting of immunoprecipitates with anti-FLAG antibody for detection of immunoprecipitated
874 DYRK1A.

875 **C.** Expression levels of GFP-FAM53C in total cell lysates.

876 **D.** Expression levels of 3xFLAG-tagged wild type and deletion mutants of DYRK1A in total cell lysates.

877

878 **Figure 5. Suppressive effect of the FAM53C binding on the kinase activity of DYRK1A**

879

880 3xFLAG-DYRK1A was expressed in COS7 cells (*lanes 2, 3, 5, & 6*) with (*lanes 3 & 6*) or without (*lanes*
881 *1, 2, 4, & 5*) GFP-FAM53C and affinity purified. As controls, mock affinity purification with control
882 resin (*lanes 1-3*) and affinity purification from non-transfected cell extracts (*lanes 1 & 4*) were included.
883 *In vitro* DYRK1A protein kinase assay was conducted with recombinant MAPT/Tau protein as a substrate.
884 In addition, Mg²⁺/ATP requirements for the kinase reactions were examined (*lanes 7-10*). Purified
885 recombinant MAPT/Tau was incubated with affinity purified DYRK1A with or without Mg²⁺ (10 mM)

886 and/or ATP (5 mM) as indicated on the top. DYRK1A-dependent phosphorylation of MAPT/Tau on
887 Thr212 and DYRK1A electrophoretic mobilities were determined by Western blotting.

888
889 **A.** Anti-phospho-Tau (Thr212) Western blotting showing the DYRK1A kinase activity to an exogenous
890 substrate MAPT/Tau.

891 **B.** CBB staining of the kinase reaction mixtures showing the amounts of MAPT/Tau protein.

892 **C.** Anti-FLAG Western blotting showing the amounts and electrophoretic mobilities of DYRK1A.

893 **D.** Anti-FAM53C Western blotting showing the association of overexpressed FAM53C with DYRK1A.
894 Endogenous FAM53C was not visible at this exposure.

895 **E.** Anti-phospho-Tau (Thr212) Western blotting showing the DYRK1A kinase activity to an exogenous
896 substrate MAPT/Tau.

897 **F.** CBB staining of the kinase reaction mixtures showing the amounts of MAPT/Tau protein.

898 **G.** Anti-FLAG Western blotting showing the amounts and electrophoretic mobilities of DYRK1A.

899

900 **Figure 6. DYRK1A-mediated association of FAM53C with DCAF7/WDR68**

901
902 HA-DCAF7/WDR68 (*lanes 1-7*) and 3xFLAG-FAM53C (*lanes 3-7*) were expressed in COS7 cells with
903 full length (*lanes 2 & 4*, DYRK1A), the N-terminal domain (*lane 5*, DYRK1A-N), the kinase domain
904 (*lane 6*, DYRK1A-K), and N-terminal+kinase domain (*lane 7*, DYRK1A-NK) of GFP-tagged DYRK1A
905 as indicated.

906
907 **A.** The amounts of immunoprecipitated FAM53C were shown by Western blotting with anti-FLAG
908 antibody.

909 **B.** The association of DYRK1A with immunoprecipitated FAM53C was shown by Western blotting with
910 anti-GFP antibody.

911 **C.** The association of DCAF7/WDR68 with immunoprecipitated FAM53C was shown by Western blotting
912 with anti-HA antibody.

913 **D.** The amounts of total expressed FAM53C in cell extracts were shown by Western blotting with
914 anti-FLAG antibody.

915 **E.** The amounts of wild type and deletion mutants of expressed DYRK1A in cell extracts were shown by
916 Western blotting with anti-GFP antibody.

917 **F.** The amounts of total expressed DCAF7/WDR68 in cell extracts were shown by Western blotting
918 (anti-DCAF7/WDR68 antibody was used for this panel due to non-specific signals observed with
919 anti-HA antibody in the cell extracts).

920 **G.** The schematic illustration of the tethering function of DYRK1A observed in **A-C**. Expressed
921 DCAF7/WDR68 (*yellow*), FAM53C (*red*), and DYRK1A [N-term (*green*), kinase (*blue*), and C-term
922 (*pink*) domains] in the Input (total cell extracts) are shown (*right*). FAM53C, bound DYRK1A, and

923 tethered DCAF7/WDR68 in the FAM53C-immunocomplexes are indicated (*left*). Lane numbers
924 correspond to the lanes shown in **A-F**.

925

926 **Figure 7. FAM53C anchors DYRK1A in the cytoplasm**

927

928 **A-E.** NIH-3T3 cells were transfected with GFP-FAM53C and/or 3xFLAG-DYRK1A. The intracellular
929 distribution of FAM53C (*left panels, green*) and DYRK1A (*center panels, magenta*) was visualized
930 by fluorescent microscopy. Concurrently, cells were stained with Hoechst 33342 for visualization of
931 nucleus (*right panels, blue*). (A) Control without transfection; (B) GFP-FAM53C alone; (C)
932 3xFLAG-DYRK1A alone; (D) Both FAM53C and DYRK1A; (E) A merged image of D. Scale bars
933 = 50 μm .

934 **F-K.** NIH-3T3 cells were transfected with 3xFLAG-FAM53C and/or GFP-DYRK1A. The intracellular
935 distribution of FAM53C (*left panels, magenta*) and DYRK1A (*center panels, green*) was visualized
936 by fluorescent microscopy. Concurrently, cells were stained with Hoechst 33342 for visualization
937 of nucleus (*right panels, blue*). (F) 3xFLAG-FAM53C alone; (G) GFP-DYRK1A alone; (H-K)
938 Both FAM53C and DYRK1A; (I) A merged image of H. (J, K) Two representative microscopic
939 fields showing cells with different expression levels of FAM53C. The arrows indicate cells with
940 high FAM53C expression and arrowheads indicate cells with low or no FAM53C expression.
941 Scale bars = 50 μm .

942

943 **Figure 8. Tethering function of DYRK1A to FAM53C and DCAF7/WDR68**

944

945 **A-D.** NIH-3T3 cells were transfected with GFP-DCAF7/WDR68 (*green*), HA-DYRK1A (*magenta*), and
946 3xFLAG-FAM53C (*blue*) and the intracellular distribution of these proteins was examined by
947 fluorescent microscopy. (A) DCAF7/WDR68 alone; (B) DCAF7/WDR68 and DYRK1A; (C)
948 DCAF7/WDR68 and FAM53C; (D) DCAF7/WDR68, DYRK1A, and FAM53C. Scale bars = 50
949 μm .

950 **E-H.** NIH-3T3 cells were transfected with 3xFLAG-DCAF7/WDR68 (*blue*), HA-DYRK1A (*magenta*),
951 and GFP-FAM53C (*green*), and the intracellular distribution of these proteins was examined by
952 fluorescent microscopy. (E) DCAF7/WDR68 alone; (F) DCAF7/WDR68 and DYRK1A; (G)
953 DCAF7/WDR68 and FAM53C; (H) DCAF7/WDR68, DYRK1A, and FAM53C. Scale bars = 50
954 μm .

955

956 **Figure 9. Binding FAM53C and Hsp90/Cdc37 to DYRK1B**

957

958 3xFLAG-DYRK1B (*lanes 5-8*) was expressed in COS7 cells with (*lanes 3, 4, 7, and 8*) or without (*lanes 1,*
959 *2, 5, and 6*) GFP-FAM53C. Cells were treated with (*lanes 2, 4, 6, and 8*) or without (vehicle DMSO,

960 lanes 1, 3, 5, and 7) Geldanamycin (2.5 μ M 4h), and the binding of FAM53C, Hsp90, and Cdc37 to
961 DYRK1B was examined by co-immunoprecipitation experiments.

962
963 **A.** The amounts of immunoprecipitated DYRK1B were shown by Western blotting with anti-FLAG
964 antibody.

965 **B.** The amounts of FAM53C co-immunoprecipitated with DYRK1B were shown by Western blotting with
966 anti-GFP antibody.

967 **C.** The amounts of Hsp90 co-immunoprecipitated with DYRK1B were shown by Western blotting with
968 anti-Hsp90 antibody.

969 **D.** The amounts of Cdc37 co-immunoprecipitated with DYRK1B were shown by Western blotting with
970 anti-Cdc37 antibody.

971 **E-H.** The levels of indicated proteins in the cell extracts were examined by Western blotting. (E)
972 FLAG-DYRK1B; (F) GFP-FAM53C; (G) Hsp90; (H) Cdc37.

973

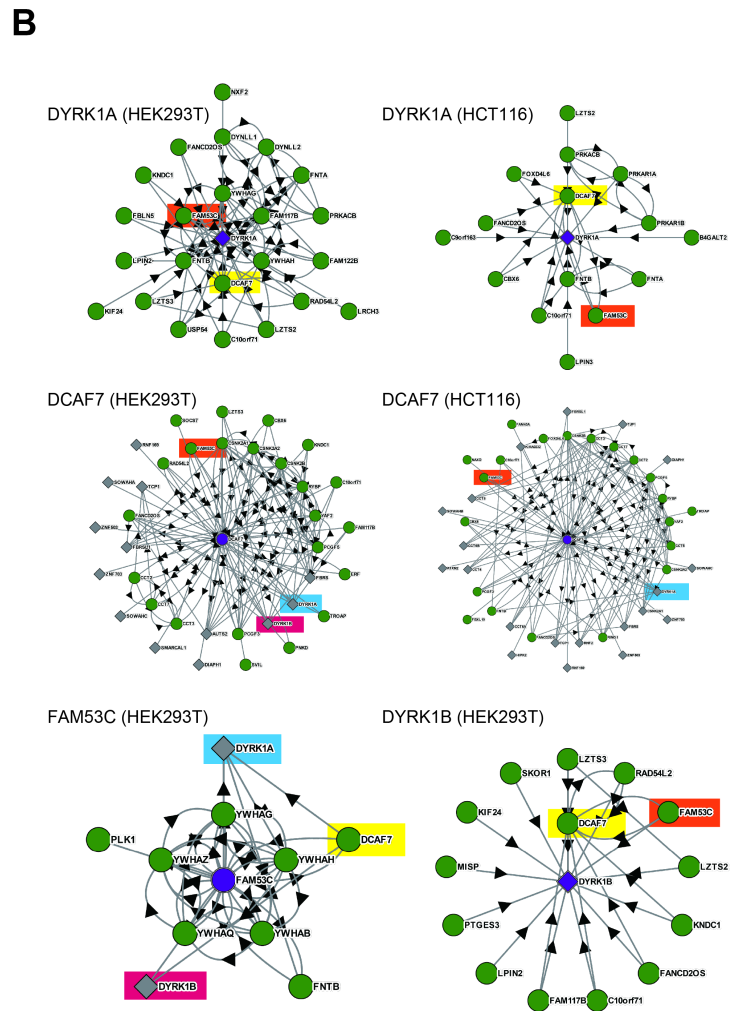
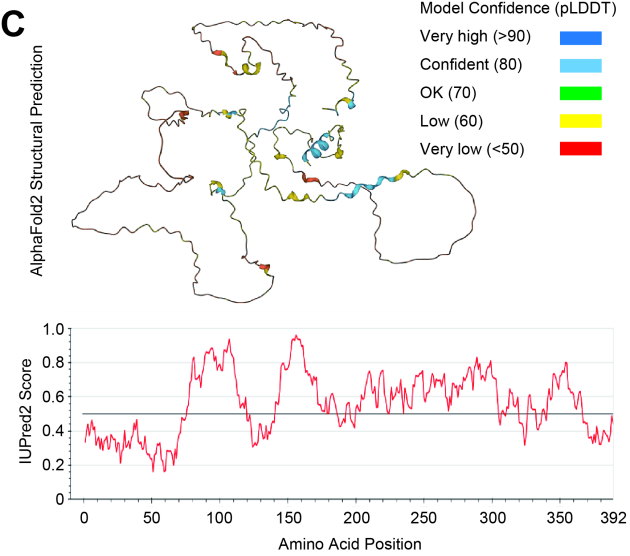
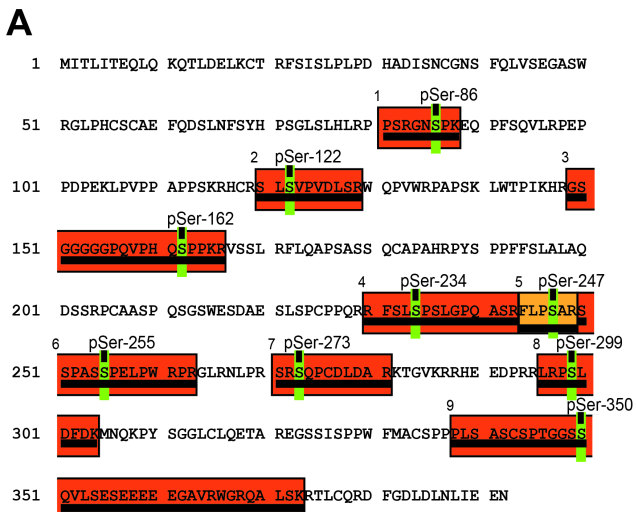
974 **Figure 10. Schematic illustrations of the suppressive anchoring function of FAM53C**

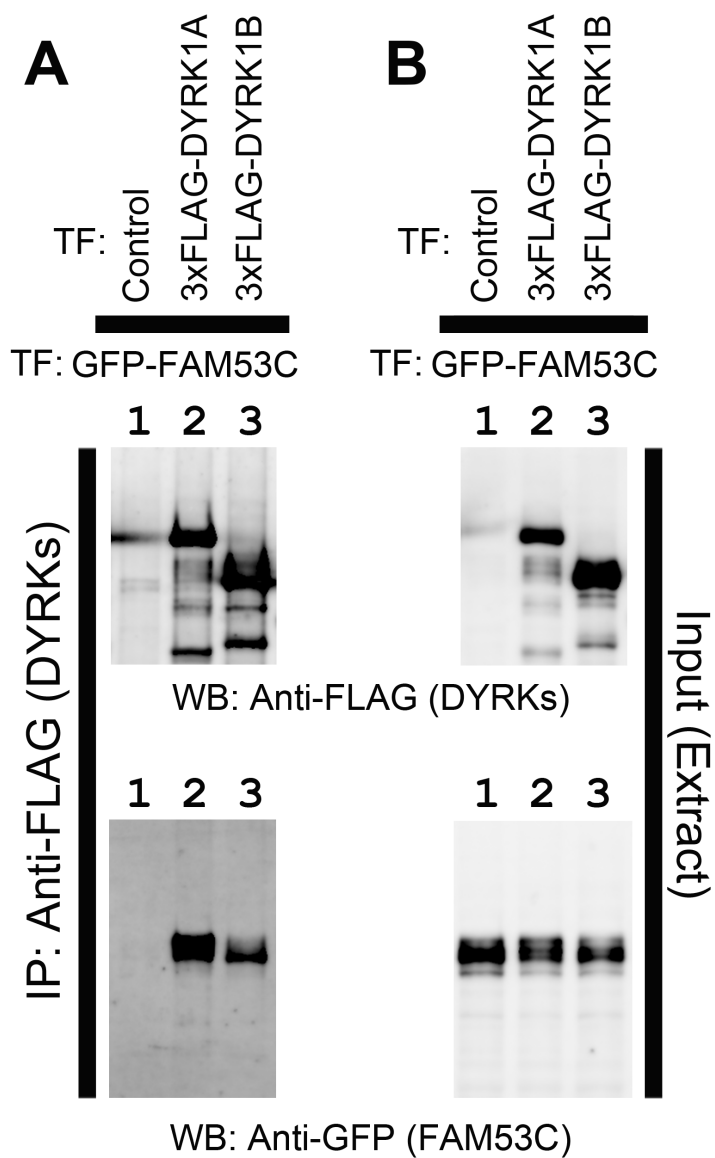
975
976 Regulation of the intracellular localization of DYRK1A by a balance between levels of DYRK1A and
977 FAM53C. Sufficient amounts of FAM53C are required for the efficient anchoring of DYRK1A in the
978 cytoplasm in an inactive state (*green area*). FAM53C-free DYRK1A is active and translocates into
979 the cell nucleus with DCAF7/WDR68 (*red area*). In certain conditions, a 1.5-times increase of
980 DYRK1A (shown by bars), by crossing over the balance threshold (shown by a boundary line), might
981 induce a drastic change of intracellular distribution of DYRK1A from the cytoplasm (*green area*) to the
982 nucleus (*red area*).

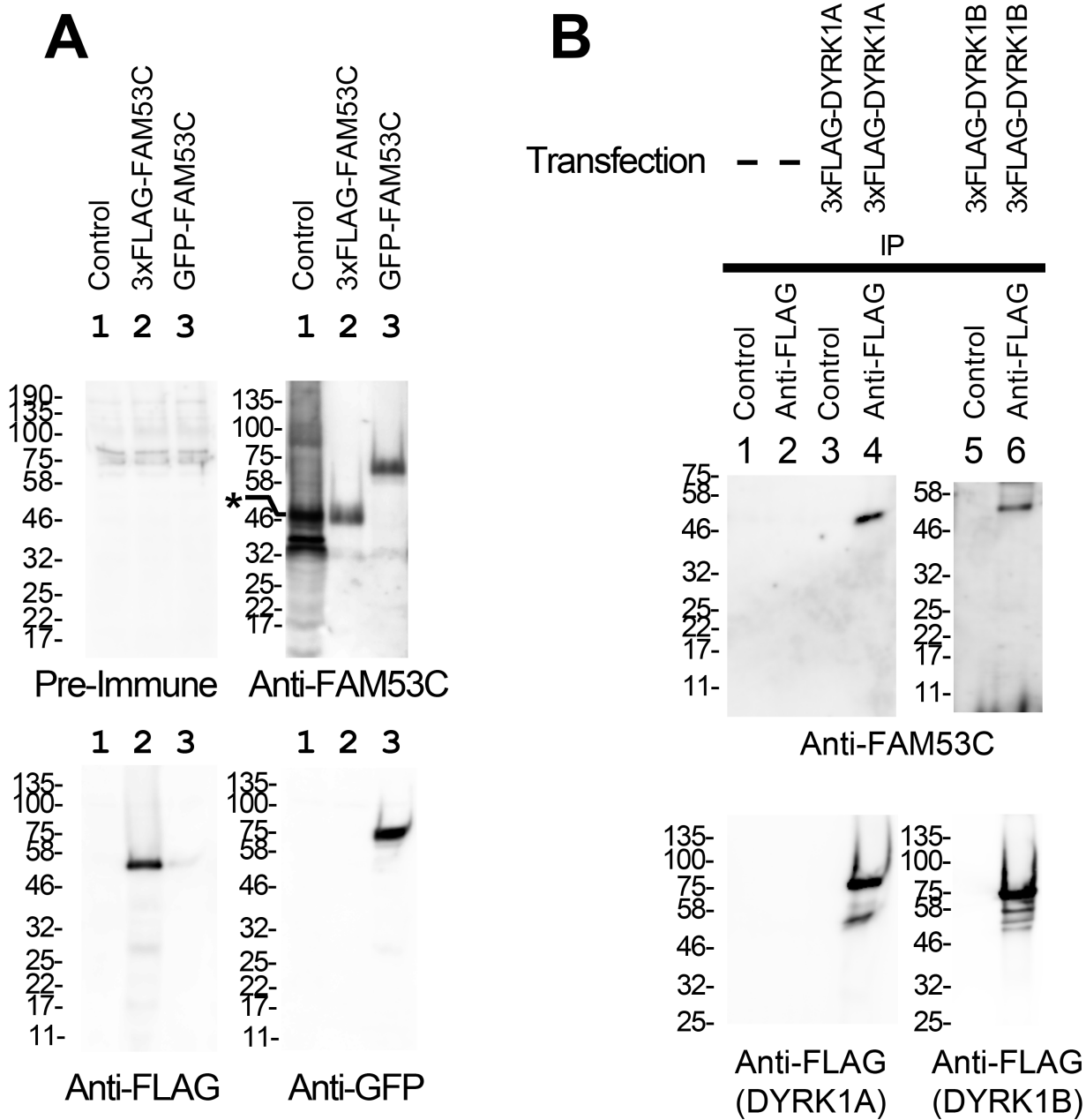
983

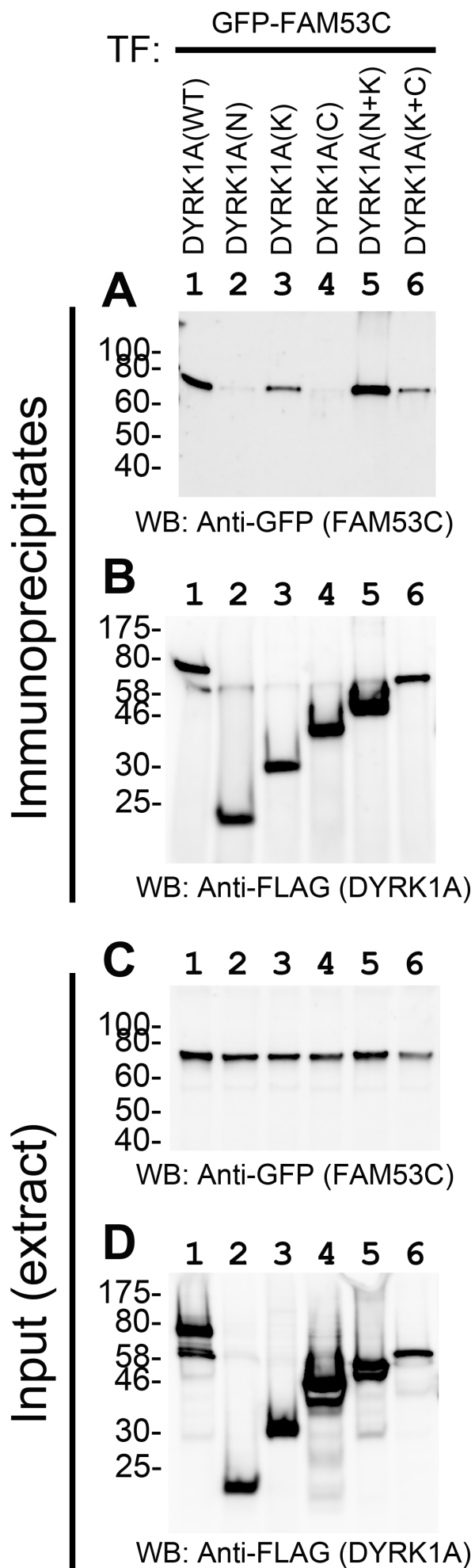
984

985



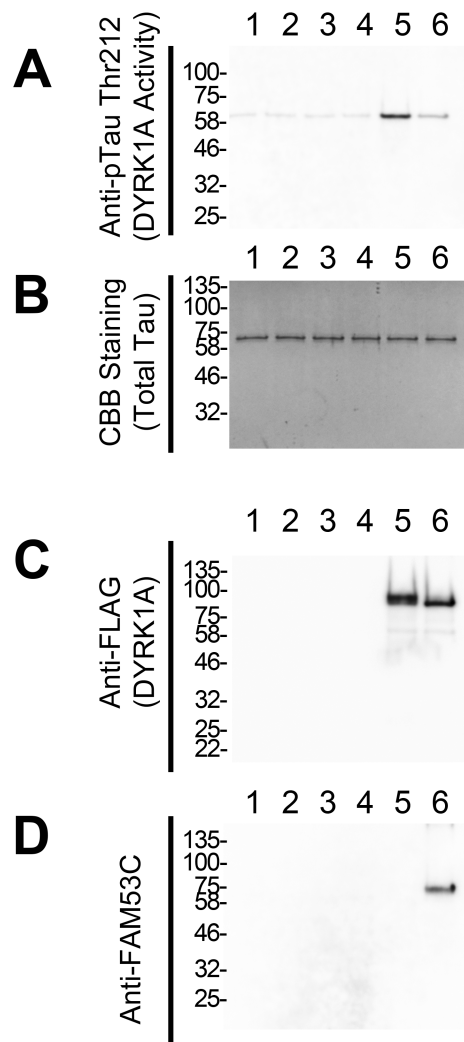




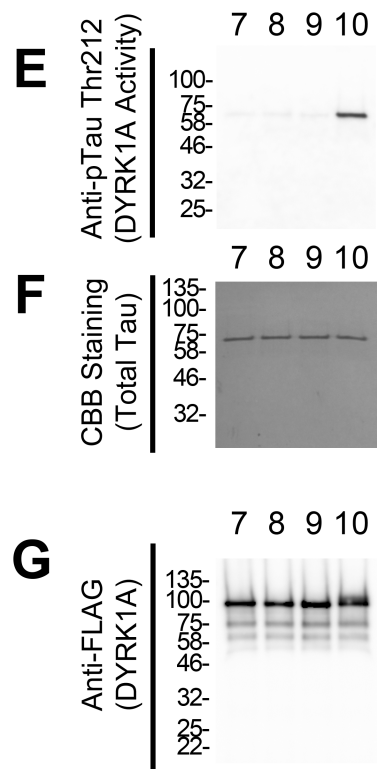


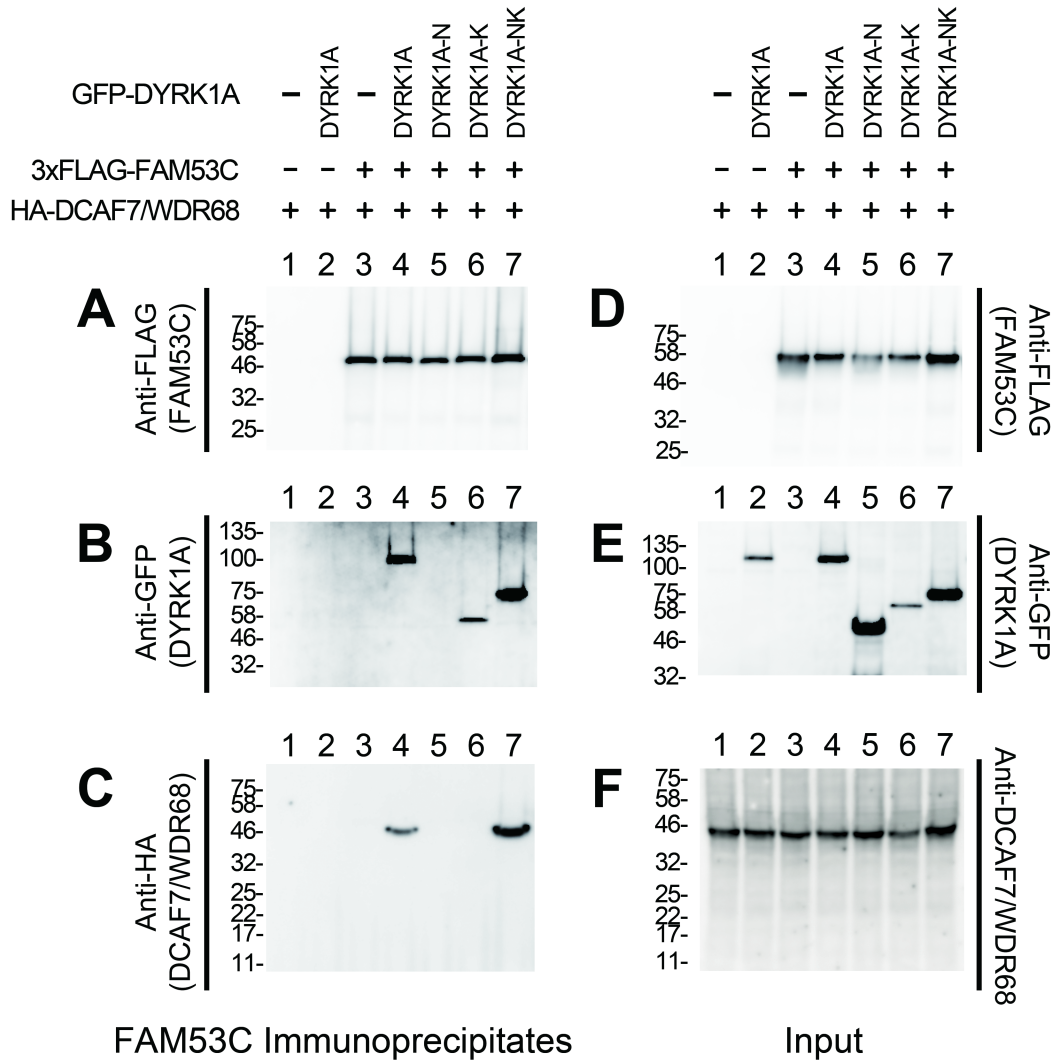
Affinity Purification: Control DYRK1A

3xFLAG-DYRK1A: - + + - + +
 GFP-FAM53C: - - + - - +

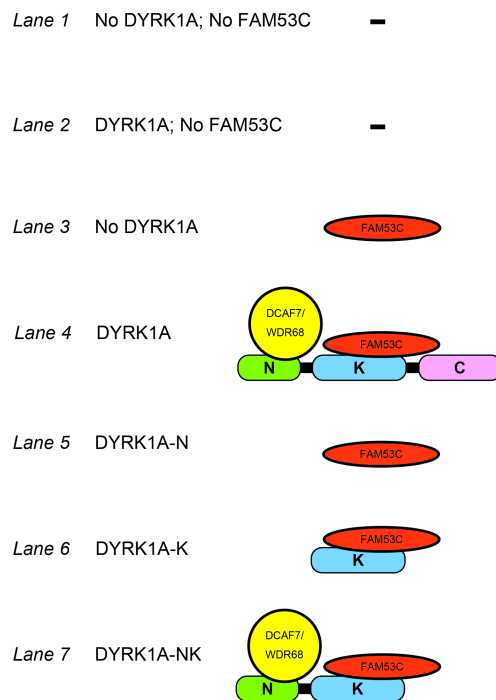


DYRK1A
 ATP: - - + +
 Mg²⁺: - + - +





G FAM53C Immunoprecipitates



Input

